Spatial Variability of Topographic Attributes and Channel Morphological Characteristics in the Ladakh Trans-Himalayas and Their Tectonic and Structural Controls

Priyank Pravin Patel, Shantamoy Guha, Debsmita Das, and Madhurima Bose

Abstract The Trans-Himalayas in India comprise of the Ladakh, Karakoram and Zanskar (also spelled as Zaskar) ranges. These ranges are marked out by the presence of several active major thrust faults, which are epicenters of recurrent seismic activity. Their alignments control the main stream courses of the area, resulting in sharp bends, obtuse junctions, steep defiles and abrupt changes in channel morphology, wherever streams transition across different morpho-structural units. The present study focuses on the drainage composition and topographic characteristics of the Leh and Nubra valleys in the Ladakh region, along the courses of the Indus, Zanskar, Shyok and Nubra rivers. The morphometric attributes and spatial variation in terrain aspects of the basins developed within the aforementioned three ranges and draining into these four rivers are examined using the ALOS PALSAR Digital Elevation Model (DEM) to elicit watershed and channel parameters related to tectonics. Thrust faults digitized from the available geological maps of the region are compared with the principal streams extracted from the above DEM dataset through an overlay analysis to discern the influence exerted by the principal thrust faults and other structural lineaments on the drainage alignment. Segment-wise stream gradient indices reveal the abrupt changes in longitudinal profile and resultant changes in channel morphological characteristics as the rivers traverse these various structural and lithological entities. These attributes of the drainage character are compared with the various lithological and geomorphic entities of the area, to elicit the river character in each physiographic unit.

Keywords Ladakh · Trans-Himalayas · Karakoram · Indus · Nubra · Morphometry · Stream gradient · Tectonics · Channel planform

P. P. Patel (✉) · M. Bose
Department of Geography, Presidency University, 86/1, College Street, Kolkata, West Bengal 700073, India

S. Guha
Department of Earth Sciences, Indian Institute of Technology, Gandhinagar, Gujarat, India

D. Das
Department of Geography, University of California, Santa Barbara, CA, USA

H. N. Bhattacharya et al. (eds.), *Himalayan Neotectonics and Channel Evolution*, Society of Earth Scientists Series, https://doi.org/10.1007/978-3-030-95435-2_3

1 Introduction

Tectonic signatures are often observed on natural landscapes that bear the marks of relative movement of the surface (England and Molnar 1990). Identifying these tectonic signatures along rivers is quite difficult since the morphological signatures are subtler, wherein the appearance of river courses and the paths taken by them from source to mouth depends on the natural setting of the environment through which they flow (Nag and Chakraborty 2003; Strecker et al. 2003). Tectonic signatures along streams can thus be identified using associative attributes like angular drainage patterns, channel sinuosity, abandoned channels, anomalous river flow, compressed meanders, abrupt change in flow directions and the asymmetry of river bends, to mention a few (Guha and Patel 2017). The strong controls exercised by the various mountain fronts all over the Himalayas are evident from the courses of the rivers that flow through it (e.g. Duncan et al. 2003). Such rivers are generally characterized by straightened courses, v-shaped valleys, asymmetric and oval-shaped watersheds and sharp knee-bend turns of seasonal rivulets and incised meanders (Burbank et al. 1996).

In this respect, the best description of the shape of a river's longitudinal profile is its slope or gradient, which is the graphic representation of the ratio of the fall of the elevation along the channel to its length over a given reach. It is thus the configuration of the channel bed or bottom in longitudinal view (Knighton 1998). In most cases and particularly in humid regions and for steady-state conditions, it is concave-upwards (Seeber and Gornitz 1983). Yet, the longitudinal profiles of natural rivers, though concave upward, rarely tend to be smooth and they often contain breaks (Oguchi 1997). Such local steepening of the channel gradient can result from one of several causes like more transitions in the lithology, the introduction of a coarser or larger bedload or from tectonic activity (Bhat et al. 2008). This 'concave up' shape of the long profile has also often been described in terms of the graded profile or profile of equilibrium for stable channels. Thus, the longitudinal profile of a river represents its long-term morphologic adjustment to the varying conditions of climate, lithology and tectonic activity (Burbank and Anderson 2011).

In a steady-state system, erosion keeps pace with uplift (Guha and Patel 2017). River gradients, which are a driving factor of erosion, are adjusted to the external forcings. Thus abrupt changes in slope along river profiles may indicate active faults encountered by these rivers (Seeber and Gornitz 1983). River channels, therefore, have a lot of controlling factors behind their evolutionary trajectories, which include topography, climate and geology. However, most often it is the tectonics of the area that plays the most crucial role of all, especially in high mountain regions. The aim of the work presented is to discern the tectonic signatures that appear in the landscape using geospatial and quantitative methods, along with their likely influence on the examined river forms in the studied area.

2 Concepts and Parameters Related to Morphotectonic Indices and River Longitudinal Profile Analysis

The availability of several of GIS technologies as well as a large range of geospatial data have led to their wide-ranging applications in geomorphology (Remondo and Oguchi 2009). These technologies allow precise quantification and mapping of geomorphic features at a range of spatial scales. Therefore, they have become an integral part of Geomorphometry, defined as the science of quantitative land surface analysis (Pike 2000; Pike et al. 2009; Sofia 2020). Geomorphometry has found applications in a variety of fields but the largest applications have been in river basin analyses (Evans, et al. 2009; Sofia 2020). A number of morphometric variables or parameters may be identified and these provide information about the land surface and hydrology of an area either in itself or in the form of indices (i.e. combinations of various parameters) (Olaya 2009; Gruber and Peckham 2009; Florinsky 2017; Patel 2012; Sofia 2020).

One such morphological parameter group includes various morpho-tectonic indices, which allow us to understand how rock resistance, tectonics and climate interact and affect the evolution of landforms and drainage in an area (Doornkamp 1986; Ramirez-Herrera 1998; Keller and Pinter 2002; Bull 2007; Brocklehurst 2010). Various morphotectonic indices have been devised over the years but the most common ones used are the hypsometric curve and integral (HI, Strahler 1952), mountain front sinuosity index (S_{mf}, Bull and McFadden 1977), valley floor to valley height ratio (V_f, Bull 1977, 1978), stream length gradient index (SL, Hack 1973), normalized stream index (NSL, Seeber and Gornitz 1983; Whipple and Tucker 2002), basin asymmetry factor (A_f, Hare and Gardner 1985), transverse topography symmetry factor (T, Cox 1994), S_t Index (Sklar and Dietrich 1998) and channel steepness index (k_{sn}, Wobus et al. 2006; Castillo et al. 2014). All these indices have been used in a number of studies dealing with tectonic geomorphology. The hypsometric integral/curve is especially important as it describes the distribution of elevations across a land surface (e.g. a basin) and the HI is the area under the curve (Strahler 1952). Based on the shape of the curve and HI values, the landscape may be divided into classical stages of youth, maturity and old, with progressively declining HI values indicating increased senility (Strahler 1952; Keller and Pinter 2002; Patel and Sarkar 2007). The skewness and kurtosis of the hypsometric curve are geomorphologically significant (Sarkar and Patel 2011) as a large, positive value of skewness indicates increased erosion in the upper reaches of a basin, whereas larger values of kurtosis indicate higher erosion in both the upper and lower reaches (Harlin 1978; Perez-Pena et al. 2008; Radaideh and Mosar 2019). However, the hypsometric curve and its integral value may also be influenced by the dimensions of the basins rather than erosion and uplift alone and Radaideh and Mosar (2019) suggested that care must be employed while using the hypsometric approach.

In contrast to the abovementioned indices that discern the tectonic influences at the landscape (basin) scale, are those which derive such information directly from the

channel itself. A river's long profile is indicative of the occurring long-term adjustments by the channel and its resultant morphology to climatic, structural, lithological and tectonic variations, perturbations and forcings. The easiest and most comprehensive way of its analysis is via methods like the Stream Length (SL) Gradient Index and its direct correlation with the geology of the study area. While the numerical calculations provide an idea about the steepness of the river, this index can be directly connected to the underlying lithology to assess the ambient stream power (Kale et al. 2010). For computing the SL Index, Hack (1973) devised a semi-logarithmic relation connecting the channel length and elevation, as:

$$H = C - k \ \ln(L)$$

where, H = elevation, L = distance from the source, C = an empirical constant and k = slope of the idealized profile, or the Gradient Index. Furthermore, a graded stream's long profile can be taken to be in a state of equilibrium and this would then appear as a straight line on a semi-logarithmic plot. Consequently, any notable deviations from the plotted or theoretically expected straight line can be taken to be indicative of forcings or disturbances along/across the stream course. Thus, Hack (1973) further provided a morphotectonic index, which is known as the Stream Length Gradient Index. This is computed as:

$$SL = \frac{(e_1 - e_2)}{[\ln(D_2) - \ln(D_1)]}$$

where, e_1 = elevation of the first point from the source, e_2 = elevation of the second point of the source, D_1 = distance of the first point from the source and D_2 = distance of the second point from the source.

The above SL index is also commonly referred to as the Stream Gradient Index (SGI). The SGI refers to a range of values that indicate the gradient of a stream. It is calculated using the fall in elevation of the stream and its change in the logarithmic value of cumulative length. Essentially, it tries to draw a relation between the amount of elevation drop and the traversed distance (Patel et al. 2021). These values are generally not bound by any range and tend to represent the geomorphic conditions of the region. Higher values are indicative of a greater change in elevation, rugged relief and steeper slopes, possibly as a result of uplift or marked variation in the local lithology (Lee and Tsai 2010), while lower values indicate flatter relief and gentler slopes. The SL to k ratio is referred to as the Normalized Stream Index (NSL) and this indicates the range of channel steepness (Seeber and Gornitz 1983; Whipple and Tucker 2002). Mathematically, it is expressed as:

$$NSL = SL/k.$$

where, SL = gradient index of a reach and k = slope of the stream's graded profile.

The NSL has a similar, if not almost identical graphs to the original SL Index and is representative of the same characteristics of the area, only reducing the scale of the values to more easily comprehendible and comparable range by dividing the originally derived values by the ideal value of the region. Seeber and Gornitz (1983) studied various Himalayan rivers and suggested that NSL ≥ 2 indicates steep reaches, whereas values >10 indicate extremely steep reaches. Since channels in tectonically active areas are generally steep, they considered SL and NSL to be indicators of neotectonics within the drainage basin. However, high SL and NSL values might also result from differential erodibility of the various lithounits (Patel et al. 2021) or mass movements like landslides, debris flows and slumps (Troiani and Della Seta 2008).

Another good indicator of the steepness or gentleness of a channel reach and the inherent effect of the local structure/tectonics/topography on the channel form is the change in the SGI or the SL change rate. In either case, a river when steeper has a greater SGI value and when gentler has a lesser SGI value. Naturally, when moving from a gentler to a steeper territory, the SGI value of the river increases and the change value calculated is a positive number. However, when moving from a steeper to a gentler territory, the river's SGI value falls as a result of which the change in SGI value returns a negative number, helping us immediately identify those places that have a significantly gentler gradient than its neighbours. It furthermore helps in correlating the reasons for such changes in gradient with the possibly concomitant changes in lithology, presence of faults and lineaments or simply the geomorphology. Using the normalized elevation and cumulative downstream distance parameters, plotted graphs can be fitted with linear, exponential, logarithmic and power form trendlines. According to Lee and Tsai (2010), when the calibre of load in the river is larger than the carrying capacity of the stream, thereby choking the river in turn, the long profile of the river has a better linear function fit. As the river downstream reaches dynamic equilibrium, it has a better exponential fit. Further downstream when the load calibre becomes even smaller, the river reaches a graded condition and the long profile is a better logarithmic fit. With increased downstream concavity of the river, the long profile fits the power function the best. Thus an indicator of the geomorphic evolutionary stage of the channel (and likely its basin) can be obtained from such trendline fitting (following Kale et al. 2010).

The various morphotectonic indices mentioned above have been used to understand the tectonic influences on landscape and drainage evolution throughout the active orogens of the world, including the Himalayas and Trans-Himalayan mountains. Seeber and Gornitz (1983) pioneered this through their work on the SGI and NSL and that paved the way for multiple studies in the region (Jamieson et al. 2004; Robl et al. 2008; Singh and Tandon 2008; Dortch et al. 2010; Phartiyal and Kothyari 2012; Mahmood and Gloaguen 2012; Dar et al. 2013; Munack et al. 2014; Kumar and Srivastava, 2017; Prerna et al. 2018; Anand and Pradhan 2019, Nag et al. 2021; Sarkar et al. 2021). Within the Ladakh region, however, such studies are somewhat limited. Dortch et al. (2010) combined the use of morphometric parameters, longitudinal profile analysis and cosmogenic radionuclide dating to conclude that the Ladakh range is eroding asymmetrically, with the southern part of the range eroding

at almost twice the rate at which the northern part is, implying that there is an imbalance between uplift and erosion in the northern catchments. The Indus basin, of which Ladakh is a part, was divided into upper, middle and lower segments through analysis of morphometric parameters and longitudinal profiles by Prerna et al. (2018), where they concluded that a third of the basin is in a state of tectonic stability. However, their finding stands in conflict with those of a recent study along a 225 km long stretch of the River Indus (Nag et al. 2021), which concluded that the upper Indus is yet to reach tectonic stability and has continued to have tectonic disturbances throughout the late Quaternary. This suggests that tectonic disturbances rather than climate driven changes are the dominant raison d'être for the present configuration of the landscape in Ladakh.

3 Study Area

Ladakh (32°15′ N–36° N and 75°15′–78°15′ E; approx. 119,820 km^2 in area) may be considered as the western extension of the Tibetan Plateau (Fielding 1996; Sharma 2003). Due to its remote location, rugged topography, inclement weather conditions and strategic position, studies on this region were scarce till the 1990s. Some notable works (e.g. Cunningham 1854; Drew 1875; Gansser 1964), nevertheless, did exist. However, the proliferation of research since the 1990s has shed a wealth of information about the geology and geomorphology of Ladakh. The entire Ladakh region may be divided into four tectonic zones, namely, from south to north, the Zanskar (or Zaskar) Suture Zone, the Indus-Tsangpo Suture Zone (ITSZ), the Shyok Suture Zone and the Karakoram Plutonic Complex (Thakur 1981). Parallel to these, run three major mountain ranges, the Zanskar Range, the Ladakh Range and the Karakoram Range. The study areas, the Leh and Nubra valleys, lie on either side of the Ladakh Range. Numerous studies have documented the glacial geomorphology of Ladakh (summarized by Dortch et al. 2013). Though glaciers in the Ladakh region only made small advances from their present positions during the Late Glacial (Owen 2011, 2014; Owen and Dortch 2014), their retreat has left a remarkable assemblage of landforms that are essentially paraglacial (sensu Church and Ryder 1972) in nature. The main components of this landscape include glacial troughs, moraines, cirques, fluvial terraces, alluvial fans, sand dunes and palaeo-lacustrine deposits (Juyal 2014).

In terms of climate, this region lies in the rain-shadow zones of successive Himalayan and Trans-Himalayan ranges, and as such the prevailing climatic conditions are typical of a high altitude cold desert. At Leh, the maximum and minimum temperature in January is −2.8 °C and −14.0 °C, while those in July are 24.7 ° C and 10.2 ° C, respectively (Osmaston 1994). Though the average annual precipitation is <500 mm (Bookhagen and Burbank 2006; Hedrick et al. 2011), the precipitation regime is affected by the altitude, the Indian summer monsoon streams and mid-latitude westerly disturbances (Benn and Owen 1998; Dortch et al. 2010, 2013). While the 30-year average precipitation at Leh is 115 mm/year, only a small percentage of it is in the form of snow (Osmaston 1994). A recent study has found

that over a period of 89 years (1901–1989), both the total annual precipitation and winter precipitation in Leh have been showing a declining trend (Bhutiyani et al. 2010). Very little climatic data exists for the Nubra Valley. However, it is distinctly colder and wetter (precipitation is mostly in form of snow) as it lies between the Ladakh and Karakoram ranges, where the temperature is below 0 °C for significant parts of the year (Bhutiyani 2014). Most of the precipitation is received from the western disturbances that hit the region during the winter months (September to April). During this period, the temperature can drop to −25 °C (Nagar and Ahmed 2007). After April, the weather improves and July is the hottest month when the temperature in the valley can be as high as 32 °C (Nagar and Ahmed 2007; Ganjoo et al. 2014).

Another climatic parameter that has an important control on geomorphic processes in Ladakh, including the two study areas, is insolation. Due to its high elevation and consequent, low temperature and pressure (510 mm of Hg at Leh [Bharadwaj et al. 1973]), the atmosphere here is rarified. As a consequence, Ladakh receives a large amount of insolation, approximately 320 days of sunshine in a year (Lohan and Sharma 2012). Ramachandra et al. (2011) found that on average, the Ladakh area receives between 4.7 and 5.0 KWh/m^2/day of insolation throughout the year, but during the summer months (May to August), the range increases to between 5.7 and 6.7 KWh/m^2/day. Additionally, Jacobson (2000) reported that during 1996–1998, Leh received 5530 Wh/m^2/day of solar energy, whereas Sumoor in the Nubra Valley received 5300 Wh/m^2/day. These studies suggest that insolation is a potent force that can exacerbate thermal weathering in the study area.

The Indus is the main river of the region. As an antecedent stream that was formed in the Eocene (Searle and Owen 1999), it initially follows the strike of the Karakoram Fault before taking a westward turn to flow along the east–west trending Indus-Tsangpo Suture Zone (ITSZ) (Clift 2002). Together with its tributaries (the Dras, Zanskar, Shyok and Nubra rivers), it forms the lifeline of Ladakh. The town of Leh (34°17′ N; 77°58′ E) is situated on the right bank of the Indus, on the southern foot slopes of the Ladakh Range. One of the longest tributaries of the Indus, the River Shyok, flows parallel to the Indus, on the northern side of the Ladakh Range, before joining it near Skardu. The confluence of the Shyok and its tributary, the Nubra, near the village of Diskit (34°33′ N; 77°32′ E) has given rise to a barbed drainage pattern due to stream piracy (Juyal 2014). The chosen study area in this paper comprises the Zanskar–Indus–Shyok–Nubra valleys and their intervening mountain ranges (Fig. 1).

4 Datasets and Methods

The present study has used several of different datasets that are listed and described below:

a. The terrain attributes of the area studied were mapped from the ALOS (Advanced Land Observing Satellite) PALSAR (Phased Array type L-band

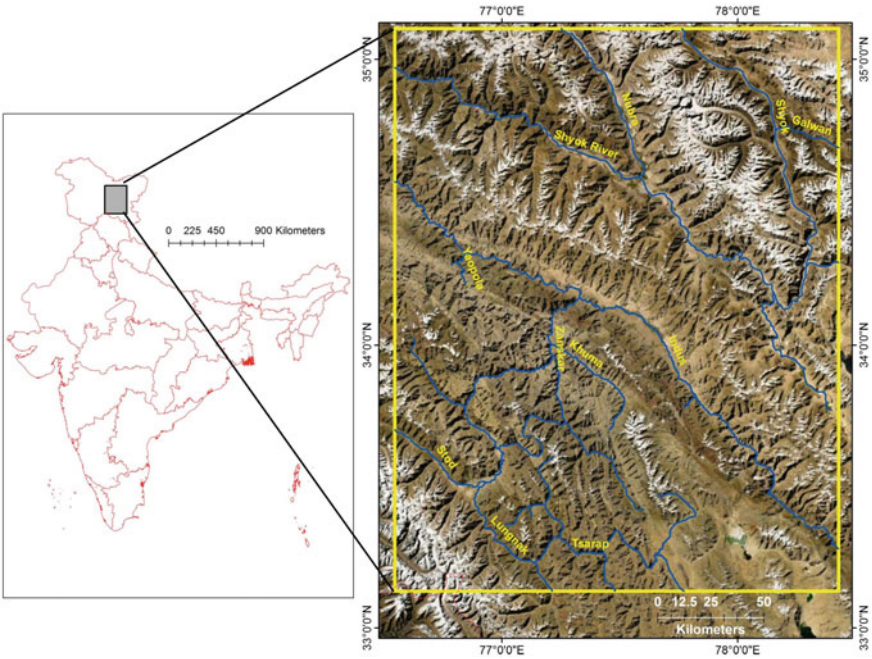

Fig. 1 Location of the study area within Ladakh

Synthetic Aperture Radar) Digital Elevation Model (DEM) of spatial resolution 12.5 m, obtained from the Alaska Satellite Facility. This is at present the highest resolution freely available global DEM (as a re-sampled by-product of the SRTM 30 m DEM) and its use was preferred since DEM resolution has been shown to have a significant effect on the terrain attributes derived (Das et al. 2016). Since this DEM is of an ellipsoidal nature, the required conversion of the elevation values from the reference ellipsoid to the required geoidal heights was done using the $1' \times 1'$ interval Earth Gravity Undulations Model (EGM2008) dataset that was interpolated for the study area. The finally corrected DEM with proper elevation values (Fig. 2) was obtained using the equation:

$$H = h - N$$

where, H = corrected elevation or orthometric height, h = ellipsoidal height and N = geoid height.

b. The corrected DEM was processed for any data gaps and voids and to remove any inadvertent data peaks and pits in the Geospatial WhiteBox software environment. Subsequently, standard D-8 flow routing and flow accumulation algorithms were used to extract the principal drainage lines and their tributary networks and perform Strahler order classification of streams (see Patel and

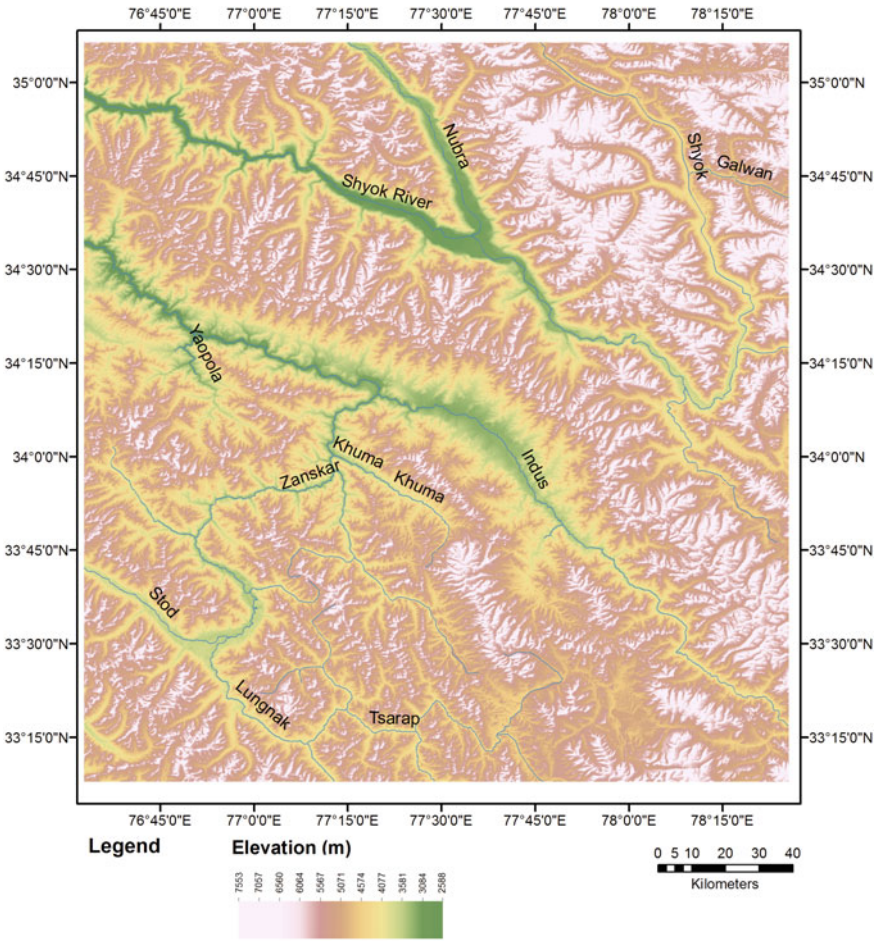

Fig. 2 The corrected DEM representing the elevation values in the study area

Sarkar 2009, 2010 for full details on these methods and their utility). The drainage basins of the ascertained stream segments (Fig. 3) were extracted using the classified flowlines and the entire raster datasets thus elicited were converted to vector shapefiles for ease of mapping and parameter extraction. Once the principal drainage lines were discerned in the above manner (i.e. the courses of the Zanskar, Shyok (its upper and lower segments, situated before and after its great bend), Nubra and Indus), we identified all the river basins that drained directly into these channels. Leaving out the very minor stream segments, all basins of Strahler Order 2 and higher (which went up to Order 5) were thus mapped (Fig. 4). In all, 177 such basins were identified and each of these were assigned a numerical code to differentiate them from each other (Fig. 5) and also the relative position of each basin (i.e. which river it drained

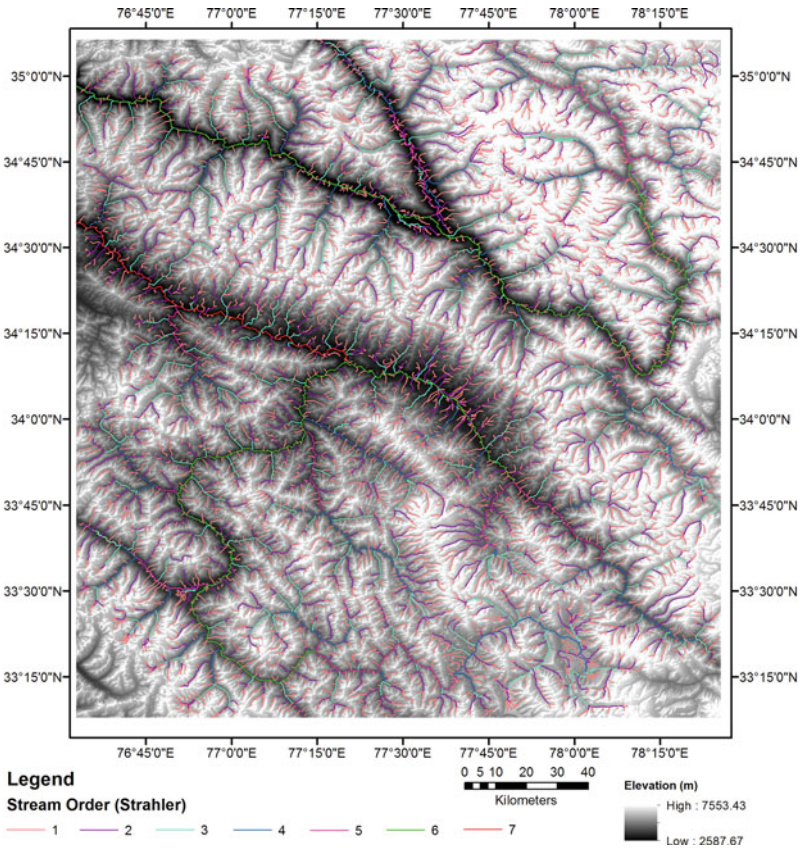

Fig. 3 Classified streams according to the Strahler (1952) stream segment ordering scheme

into and whether its location was on the right or left flank of the main channel) was ascertained and input into its respective database (Fig. 5).

c. A range of terrain parameters were directly extracted from the DEM and enumerated for each of the river basins. These comprised of the maximum, minimum and mean basin elevation and its standard deviation, the mean basin slope, hypsometric integrals, ruggedness and dissection indices (for details of their enumeration methods see Patel 2012, 2013 and Sarkar and Patel 2009, 2012). Alongside these, the basin geometric attributes (area and perimeter) and shape (circularity ratio) were also computed. Enumeration of the basin-wise stream frequency and drainage density parameters was done by overlaying the stream segments on each basin and clipping their extents, followed by stream number counts and total length estimates.

d. The reach-wise channel steepness index (SL index) was measured and mapped for the principal rivers, using the method outlined in the prior section. It is to be noted that some of these streams are international rivers and as such only a

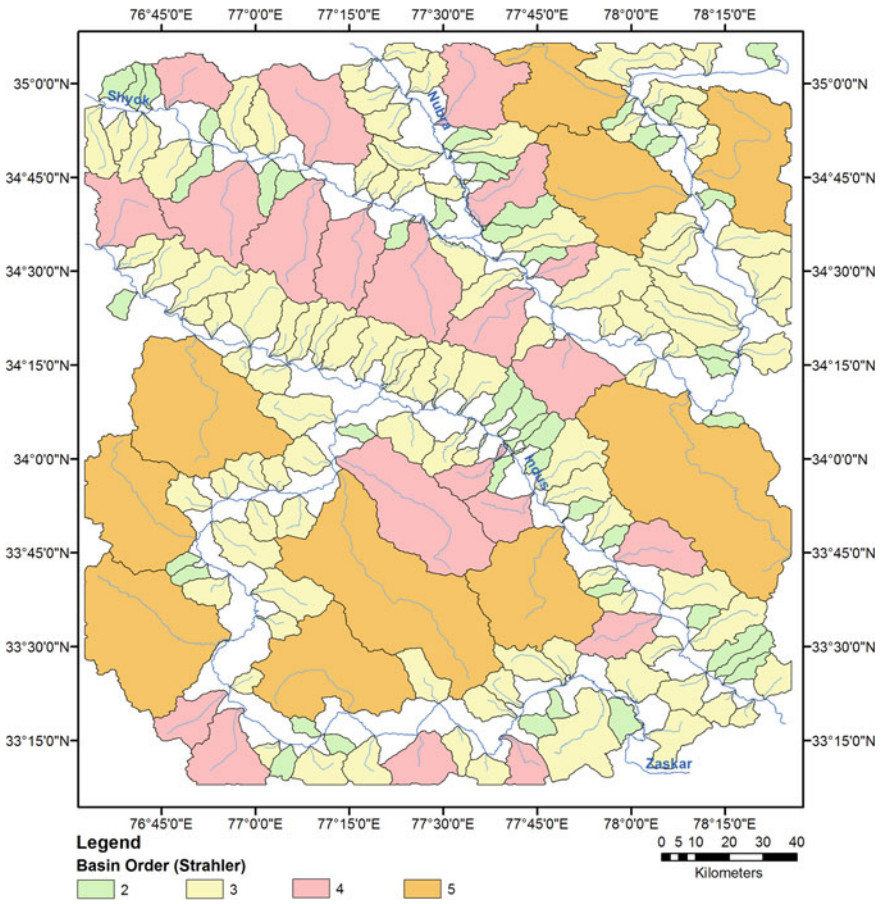

Fig. 4 The demarcated basins of Strahler second order and higher that drain directly into the four principal drainage lines of Indus, Shyok, Nubra and Zanskar

portion of their courses lie within India. Therefore instead of looking into the longitudinal profile character of the whole stream, we have constrained ourselves to simply examining it within the demarcated study area, in which these river valleys are in close juxtaposition to each other. The long profiles of these partial courses were extracted from the corrected DEM and an 11-pixel smoothening window (following Kale et al. 2010) was used to remove any irregularities in their plots. Each stream was divided into segments of 5 km each for the SL Index enumeration. This created 66 segments for the Indus, 105 segments for the Shyok (comprising its upper and lower portions, before and after its great bend within the study area), 24 segments for the Nubra and 82 segments for the Zanskar. Subsequently, their respective fall in elevation was calculated and each segment slope was found out, with a combination of these eliciting the SGI

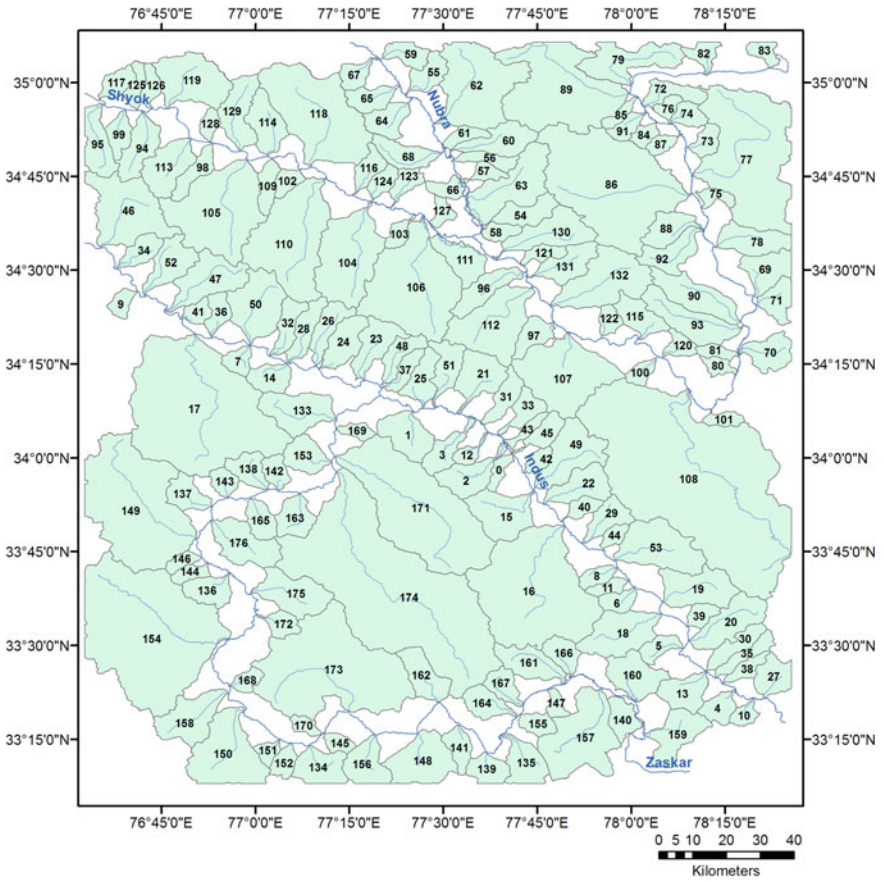

Fig. 5 The coded drainage basins for subsequent morphometric analysis

value per segment of the river. When overlain on the DEM and geological maps, a clear insight into the possible role of the lithology/structure on the channel morphology could be ascertained.

e. Breaks along the longitudinal profile are indicators of lithological or structural changes. In order that the studied rivers could be compared, despite their different lengths and different elevation differences along their courses, a normalization or standardization procedure was applied (cf. Guha and Patel 2017). Four mathematical functions were then used to compare and derive a best-fit curve on the respective profiles to ascertain the stage of development of the respective basins, as well as inculcate a process-based understanding, as previously described (cf. Kale et al. 2010).

f. Langbein's (1964) Concavity plots were used to further the argument about the shape of the river longitudinal profile curves. According to this concept, when the value is 0, the channel is straight. As the value increases, the channel starts

to curve or meander and the calibre of its load tends to decrease. The greater the relief of a given basin, the straighter the profile. Simply put, the greater the length of a basin for a given relief, the more concave it is and the river is characterised by an increase in discharge downstream with relative crustal stability.

g. A number of topographical and geological maps were used to obtain the surface lithological attributes. The toposheets of the area were obtained from the US-AMS collection and were at 1:250,000 scale. The geological maps were obtained from the Geological Survey of India (GSI) Quadrangles and the information present in these sheets were mapped and overlain on the DEM derived parameters for visual correlations.

h. High-resolution Google Earth images, in planform and tilted 3-D views, were used to examine the minor geomorphic units present in the study area. For select reaches of the principal streams, their respective stream corridor morphologic attributes (cf. Banerji and Patel 2019) could thus be ascertained and using similar information present in the GSI maps, these were outlined.

5 Results and Discussions

5.1 Ambient Structural and Geologic Characteristics

The study area reports elevations ranging from 2588 to 7553 m (Fig. 2). This almost 5000 m elevation change within this region markedly influences the terrain character and geomorphic attributes. This great elevation difference is a result of Himalayan and Trans-Himalayan tectonics and repeated movements that characterise the entire region (Burbank and Anderson 2011). The Zanskar cuts across the mountain range that bears its name while the Ladakh Range forms the water divide between the Indus and Shyok rivers, with rivers draining its southern face flowing into the Indus and those arising on the northern flanks eventually meeting the Shyok. The Great Karakoram Range abuts between the Shyok and Nubra valleys and carries on further to the east.

A number of lithologic groups and formations are present herein (Fig. 6), with all of them exhibiting a linear pattern, aligned from NW–SE, highlighting both the compressional tectonics that have occurred here, resulting in a series of parallel ranges and the melange of rocks that have been crumpled and uplifted along the main suture zones that trend in the aforementioned direction. A greater heterogeneity of these rock groups/formations is apparent in the Zanskar zone, on the left flank of the Indus. Typical metamorphics and crystallines associated with continental subduction and suture zones (ophiolites and acidic intrusives) abound. Notable is the presence of patches of undifferentiated recent sediments (mixture of coastal, glacial, aeolian and fluvial origin). This denotes the complex evolutionary history of the area and these sediment patches occupy locations where the valley floors have broadened out to accommodate them, resulting from the infilling taking place along the suture

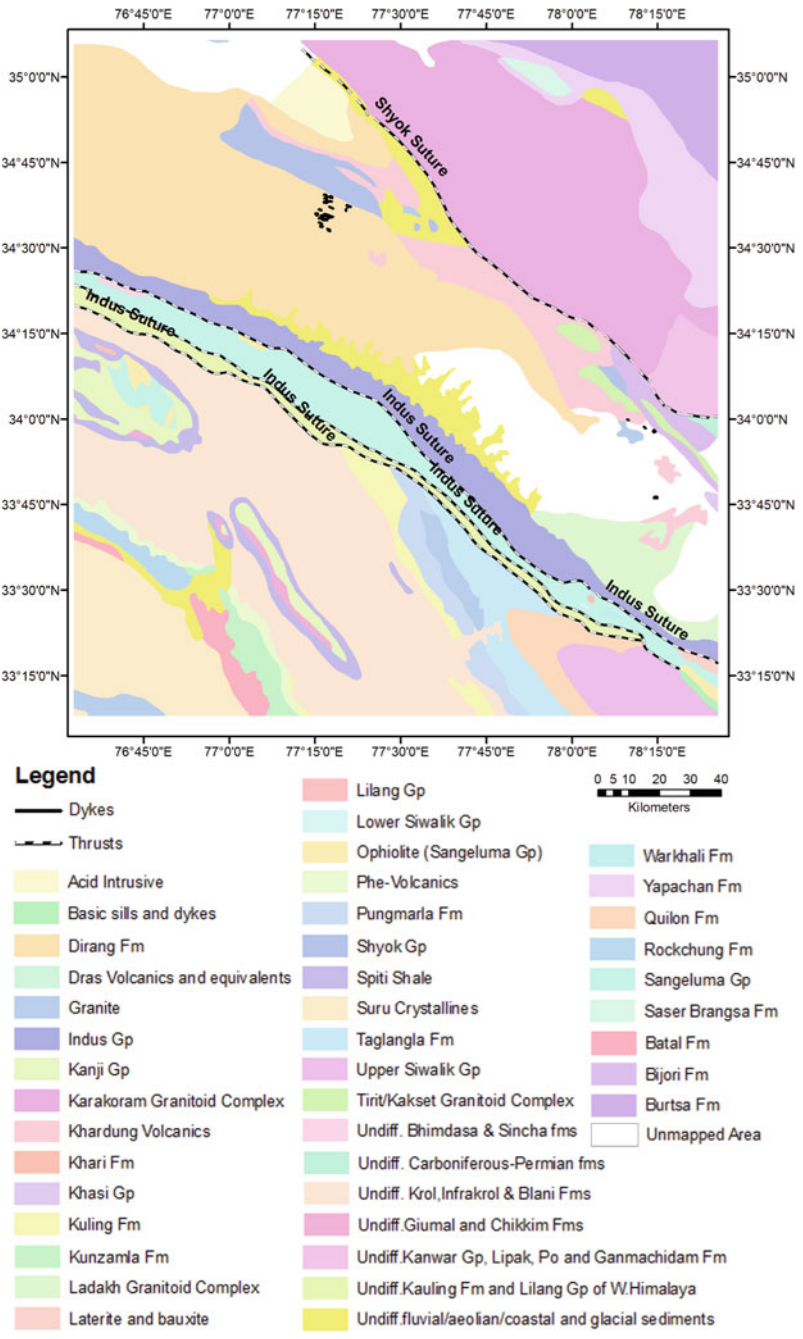

Fig. 6 Major geological formations and rock groups in the study area

zones (especially the Indus and Shyok sutures). These valley fills extend upslope as finger-like projections that represent the tributary valleys (Fig. 7) that meet these main drainage lines, as can be seen prominently along the Ladakh Range and on the eastern flank of the Nubra. By bringing rocks of very different geologic ages in close juxtaposition, these two suture zones typify the sharp lithological changes that

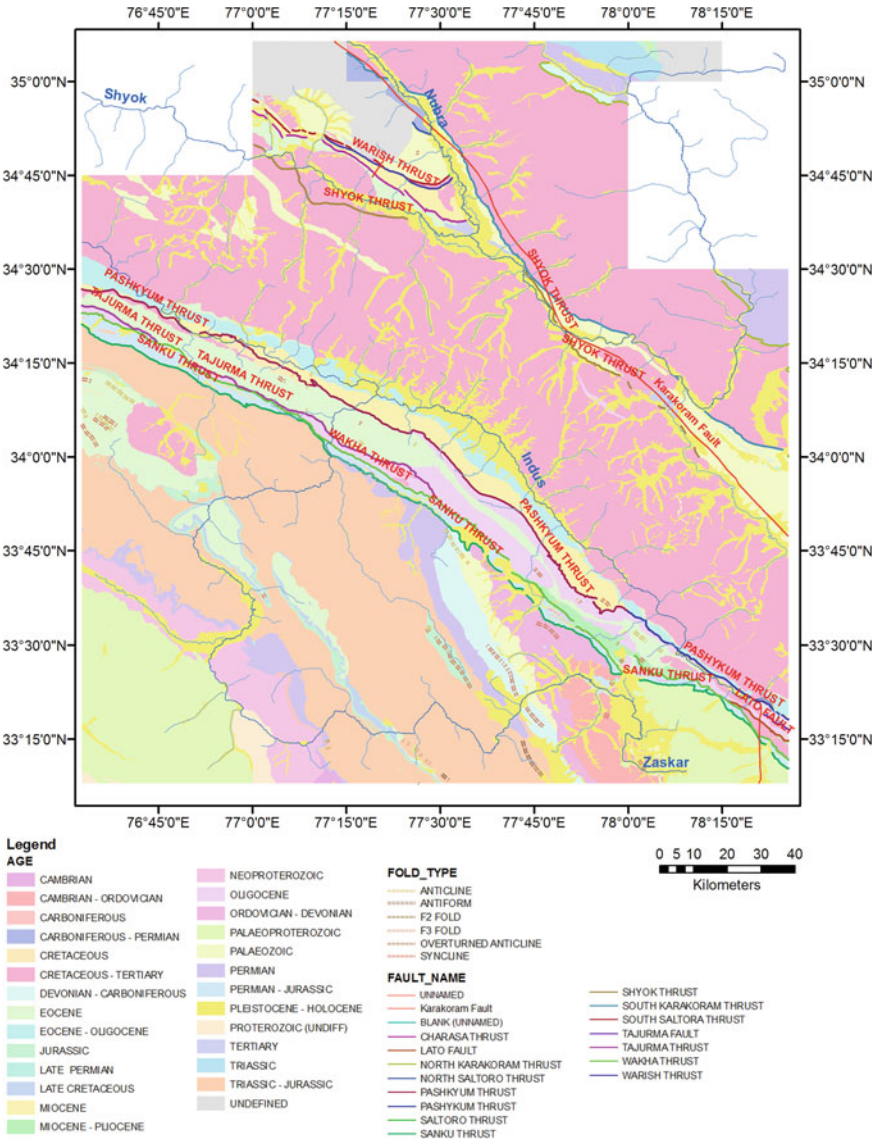

Fig. 7 Geological time periods when the constituent rock formations developed and major structural elements

are characteristic of continental subduction zones and the associated chaotic rock complex. A classic example of the intense upwarping and tilting of the constituent rocks is seen along the Indus' left flank at Stok and Choglamsar, with seemingly large-scale uniclinal and folded formations being present here (see Fig. 26k).

Such intense rock décollement also gives rise to multiple faults and folded structures alongside the main sutures and these are seen abundantly in the study area, with a variety of anticlines, synclines and folded forms present along with series of different thrusts, lineaments and faults. Simple visual comparison of their position and alignment with the overlain drainage lines makes it apparent that they exert marked control over the courses of not only the main rivers but also influence the formation of structural meanders, obtuse tributary junctions and sharp course changes throughout the entire drainage network of the area (Fig. 8). In the northern part of the map, the upper section of the Shyok initially flows to the south but then executes a sharp turn of more than 90° towards the NW on meeting the Karakoram Fault. This confined channel then courses towards the NW and occupies the Shyok Suture and then the Shyok Thrust further to the west. The alignment of the Shyok's main tributary, the Nubra, is entirely controlled by the NW–SE trending Shyok Thrust that results in these two rivers forming a remarkable obtuse barbed junction at their confluence. In the central part of the area, the course of the Indus is also constrained and controlled by the adjacent SE-NW trending Indus Suture and its associated Pashkyum, Wakha and Tajurma Thrusts (cf. Phartiyal et al. 2005; Kumar and Srivastava 2018). While the Zanskar region does not have any of the markedly developed thrusts, it has a number of folded and structural lineaments that have influenced the alignment of the main channels and its tributaries. That these faults are quite active and have influenced tectonic movements in the recent past also becomes clear when the seismicity map of the area is examined (Fig. 9). The NE and SW zones of the study area have a preponderance of earthquake epicentres. Most of these are shallow focus earthquakes and are generally above 4 MW, reflecting the ongoing tectonic movements in this area.

5.2 *Spatial* V*ariability of* B*asin-*W*ise* T*opographic* A*ttributes*

The mapped basins draining directly into each main channel were examined next. Of the total of 177 such basins that are of Strahler second to fifth orders, 54 drained into the Indus (19 on its left flank and 35 on its right), 44 into the Zanskar (26 left and 18 right), 64 into the Shyok (30 left and 54 right) and 15 into the Nubra (10 left and 5 right) (Table 1). The markedly unequal distribution of drainage basins on either flank is possibly due to the respective alignments of the main water divides and the courses these streams have cut through them. The mean basin size is 158.52 km^2 with the Zanskar region reporting the highest mean basin size and the Nubra the lowest (Table 1).

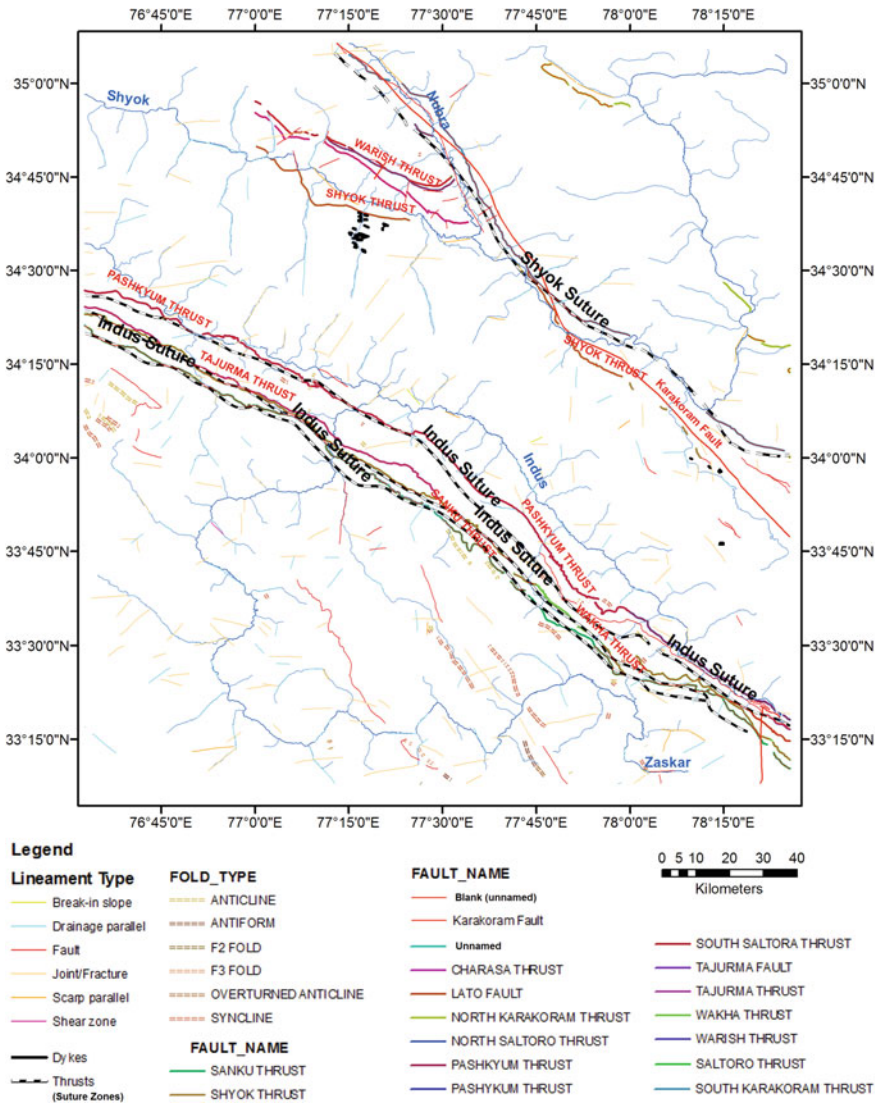

Fig. 8 Different types of structural elements present in the area and their overlay with drainage lines

We observed that the basin-average relief varies between ~1000 m and 4000 m (Fig. 10). The highest relief is observed in the northern part of the region along various tributaries of the Shyok and Nubra rivers. These regions exhibit high relief because there are topographic and chronological signatures of the displacement along the Karakoram Fault (Phartiyal et al. 2005; Imsong et al. 2017). The high standard deviation among the elevation values (Table 1) within each basin (these are often

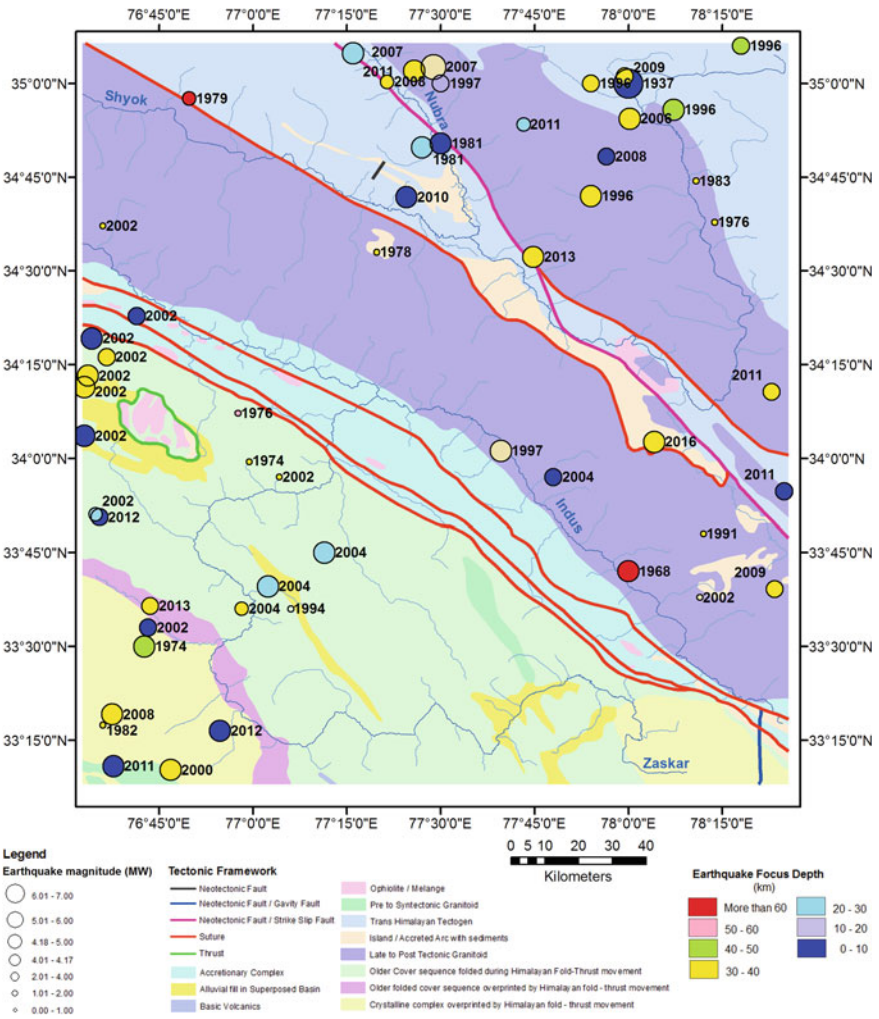

Fig. 9 Recent seismicity map of the area

1/4th or 1/5th of the mean basin relief) indicates the rugged nature of the terrain and the marked changes in elevation (and consequently surface slope) within short distances. The basin-average slope varies between 7° and 35° (Fig. 11), however, its spatial variability is not distinctly discernable. We observed that the basin-average slope is mostly high in the entire region whereas it is highest in the tributaries of the Zanskar in the southwest part and the tributaries of Shyok in the northeast part of the region. It is clearly observed that the basin-average slope is highest in the small tributaries across the region. Usually, the slope values are derived locally from the neighbourhood analysis that inherently introduces a scale-factor dependent on the

Table 1 Mean values of select morphometric parameters enumerated for basins in the Leh–Nubra region

Basin location	No. of basins	Area(km^2)	Perimeter (km)	Circularity ratio	Mean Elevation (m)	Basin relief (m)	Std. dev. elevation (m)	Avg. stream nos in basins
All basins	177	158.52	75.22	0.27	4879.80	2572.12	514.83	41
Indus all	54	123.40	69.58	0.26	4657.71	2500.80	542.65	32
Indus left Flank	19	158.52	75.22	0.27	4879.80	2572.12	514.83	41
Indus right flank	35	99.61	69.03	0.25	4630.70	2507.24	561.33	25
Zanskar all	44	198.21	78.77	0.30	4805.27	2098.48	415.16	52
Zanskar left flank	26	161.82	70.26	0.32	4779.46	2084.16	417.58	42
Zanskar Right Flank	18	250.77	91.07	0.28	4842.53	2119.17	411.68	65
Shyok all	64	175.02	79.32	0.26	5089.10	2813.48	535.41	45
Shyok left flank	30	223.90	87.40	0.27	5007.22	2825.00	556.20	55
Shyok right flank	54	131.88	72.19	0.25	5161.35	2803.33	517.08	36
Nubra all	15	98.17	67.63	0.24	5004.98	3188.37	619.22	26
Nubra left flank	10	113.32	72.90	0.23	5026.53	3268.78	642.24	30
Nubra right flank	5	67.88	57.10	0.26	4961.89	3027.56	573.18	19

(continued)

Table 1 (continued)

Avg. total stream length (km)	Stream frequency (no./km^2)	Drainage density (km/km^2)	Mean slope (°)	Std. dev. slope (°)	Ruggedness index	Dissection index	Hypsometric integral
79.59	0.26	0.50	26.65	11.76	1.29	0.42	0.53
62.65	0.27	0.52	25.29	10.42	1.30	0.43	0.53
79.59	0.26	0.50	26.65	11.76	1.29	0.42	0.53
50.88	0.25	0.52	25.28	10.38	1.29	0.43	0.53
95.90	0.25	0.47	26.12	10.62	0.97	0.36	0.48
79.02	0.25	0.46	26.59	10.84	0.96	0.36	0.48
120.30	0.26	0.47	25.44	10.30	0.99	0.36	0.47
88.23	0.26	0.49	28.09	12.94	1.39	0.45	0.57
108.55	0.26	0.48	27.88	12.27	1.36	0.46	0.57
70.31	0.25	0.50	28.27	13.54	1.42	0.44	0.57
55.88	0.25	0.55	26.98	14.93	1.79	0.50	0.57
64.37	0.24	0.55	26.61	14.28	1.82	0.50	0.57
38.91	0.28	0.57	27.71	16.22	1.73	0.48	0.56

Source Enumerated by the authors

spatial resolution of the dataset. Therefore, the hillslope dominated regions primarily depict higher slope, which is consistent in the study region.

Basin circularity ratio values are all on the lower side (all values are below 0.50) (Fig. 12). Higher values, nearer 1.00, indicate a more circular and developed basin with well-integrated drainage lines and usually having a dendritic drainage pattern developing over gentler terrain. These lower values again indicate the ambient structural control and segmented, parallel linear drainage lines that have developed on the steep flanks of the intervening high mountains between the main rivers. Overall, drainage density values are again on the lower side, possibly due to the scant rainfall received in this region. Relatively, drainage density is highest in the tributary basins of Shyok and Nubra in the northeast part of the region (Fig. 13). However, high values are also observed in the tributary basins of the Indus. The major rivers are generally oriented according to the main tectonic structures (e.g. Karakoram Fault and Indus Suture). Therefore, the relative movement of these structures results in disturbances in the tributaries of these rivers. Previously, researchers have characterised the slope angle as a factor of drainage density (e.g. Schumm 1956). However, high-resolution DEM studies have suggested that direct correlation seldom exists and corresponds to the channelization stages (Lin and Oguchi 2004). We also observed that there is no direct relationship between drainage density and the mean basin slope.

The basin hypsometric integral (HI) values again attest to the predominantly youthful nature of the landscape. Most of the HI values range between 0.4 to 0.6

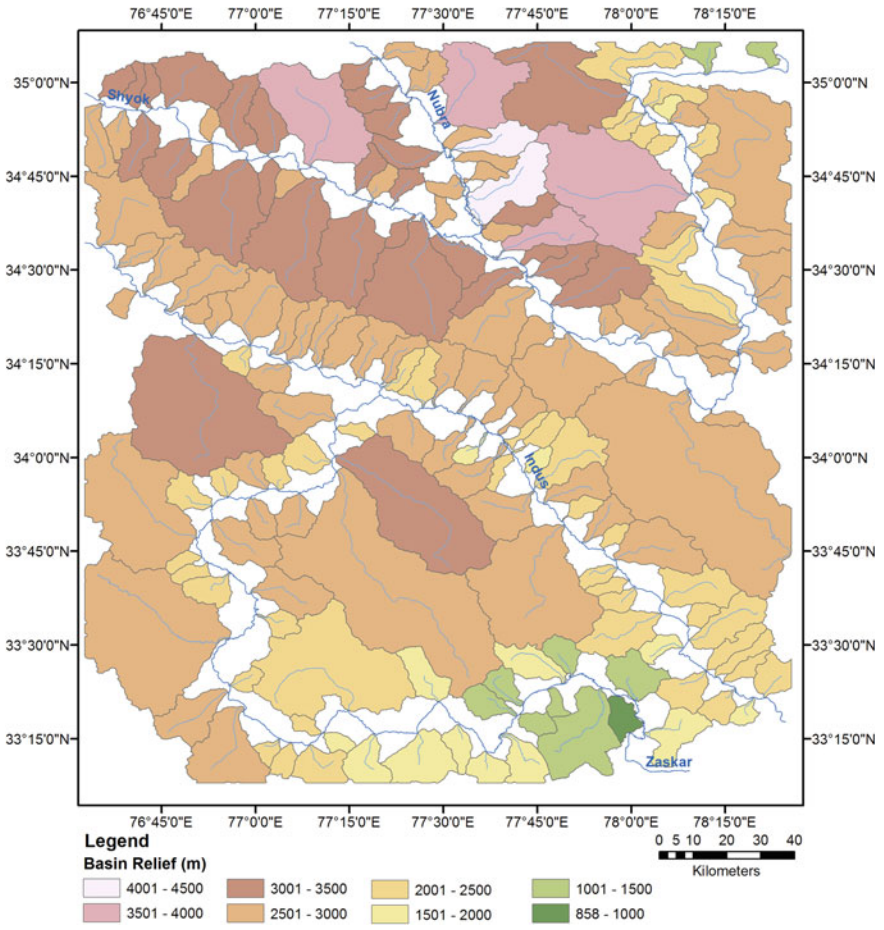

Fig. 10 Basin Relief Map

or between 0.6 to 0.8 (Fig. 14), with these higher values indicating a landscape that has suffered relatively less net dissection (uplift and/or incision). A strong spatiality is observed in this aspect. The basins flanking the Karakoram Range between the Shyok and Nubra valleys show higher values, as do the basins located around the remarkable great bend of the Shyok in the eastern part of the study area (see Table 1 for comparison of region-wise mean HI values for the constituent basins). Most basins of the Indus and Zanskar region show values between 0.4 - 0.6, being in the mature stage of geomorphic evolution. The fact that these basins still report such higher values from landscapes that are essentially millions of years old, amply attest to the ongoing uplift and increase in surface elevation that has occurred here over millennia. Consequently, the mean ruggedness index and dissection index values are also greater for the basins along the Shyok and Nubra in the northern part of the

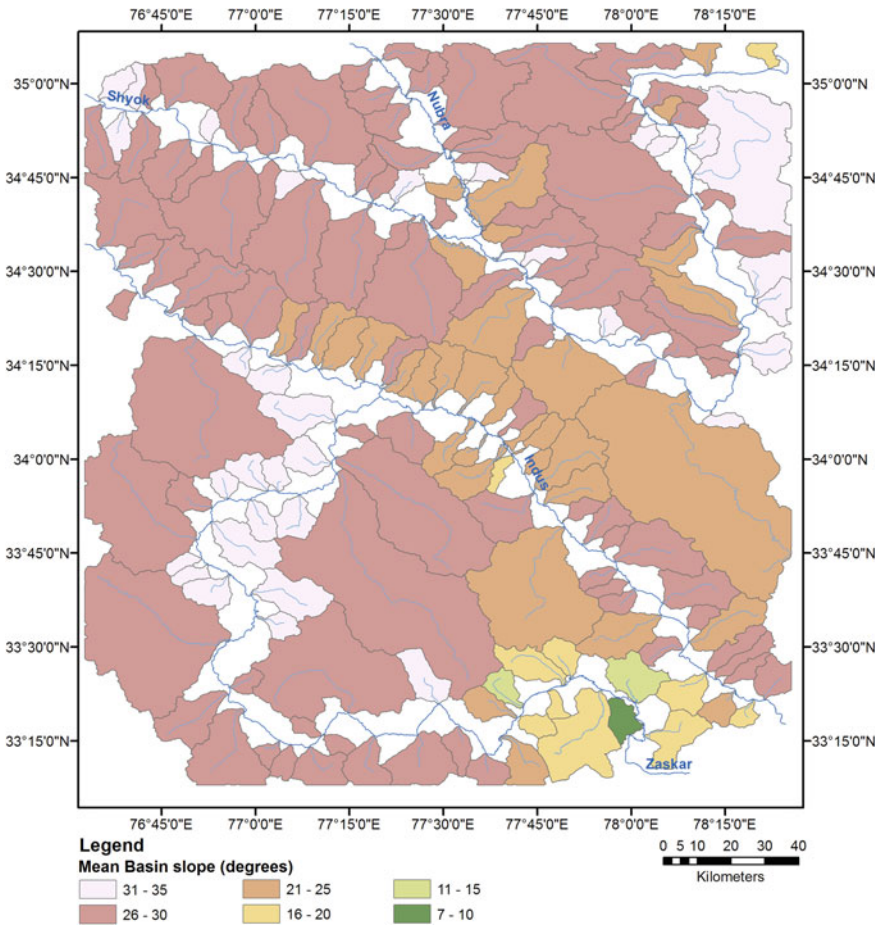

Fig. 11 Mean Basin Slope Map

study area (see Table 1 for comparison) than for the basins in the central part along the Indus or in the southern portion within the Zanskar's province.

The respective basin morphometric parameters were collated for all the 177 basins and a hierarchical clustering analysis was done through a dendrogram (Fig. 15). We could identify some distinct groupings of the basins in this manner (Fig. 16), based on the respective basin morphometric parameters. In all, 23 such basin groups were differentiated (see Table 2 for details). Most basin groups are situated on any one flank of the different ranges and water divides that cut across the study area (e.g. Groups I1, I2, M). These groupings further reveal the possible influence of the local structural elements, lithology and basin position/alignment on its formed geometric and morphological attributes.

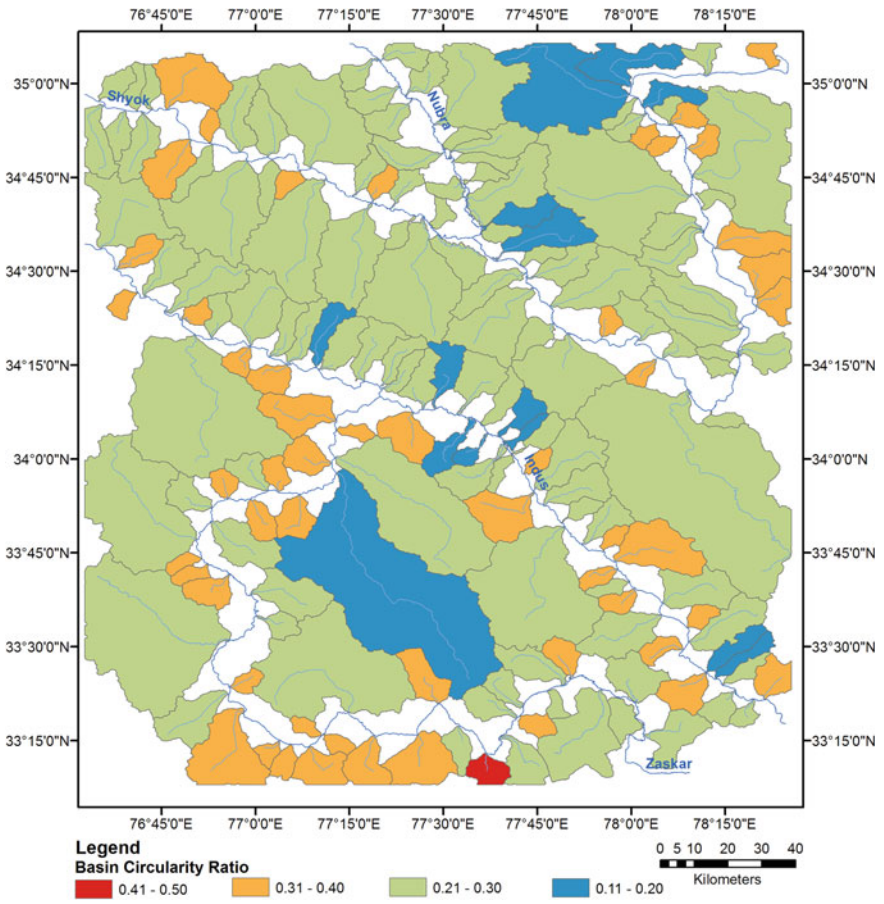

Fig. 12 Circularity Ratio values for the mapped basins

5.3 Long Profile *Characteristics of the* Main Rivers

The longitudinal profile of a river is highly sensitive to changes in the underlying lithology over which it courses or to any sudden relative elevation change arising from tectonic disturbances (Lin and Oguchi 2006; Ambili and Narayana 2014). SL index changes generally indicate the elevation drop per unit length in a region. Higher values mean that the slope is steeper while a lower value means that the slope is gentle. Sudden changes in values are indicative of tectonic occurrences, often where knick-points are located or other anomalies take place. Knick-points are longitudinally steepened sections of river reaches that bear the unmistakable signatures of tectonic activities among other factors (they can also arise due to lithological variations). They cause an abrupt change in the downstream gradient of the river and have a

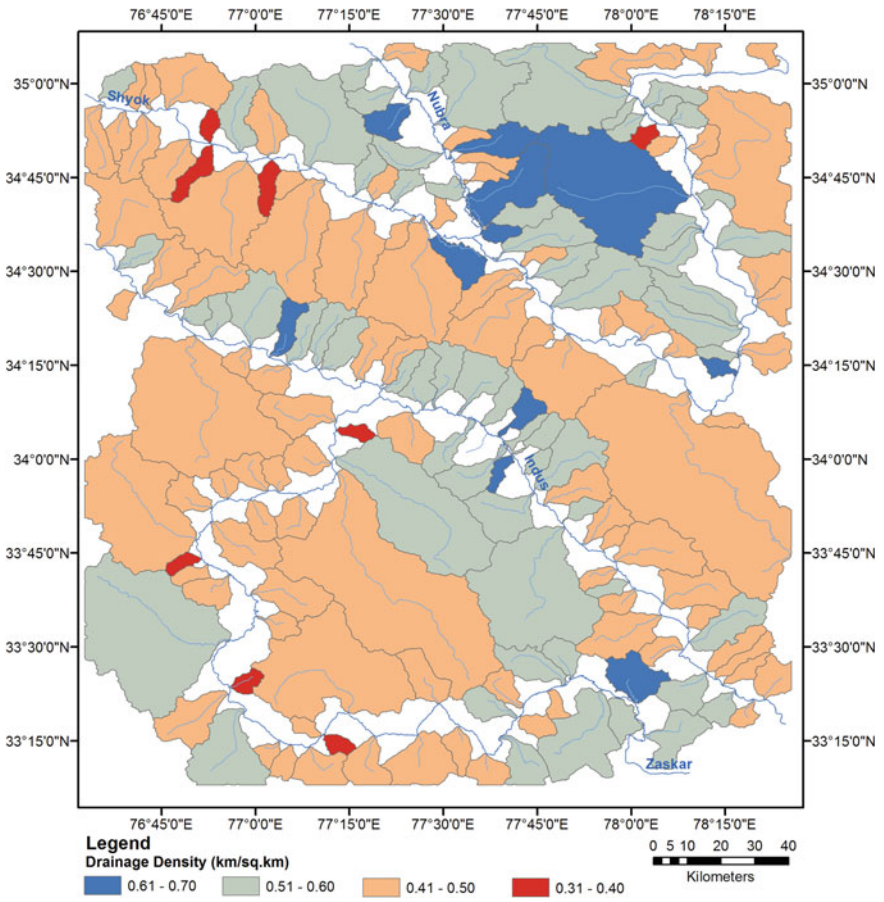

Fig. 13 Basin-wise Drainage Density Map

direct effect on the local base level of the area. Knick-points are thus a source of identification of change in a transient landscape.

Calculating the stream gradient index and the normalised stream gradient index along with their rate of change and fitting the resultant curves reveals the extent and result of the tectonism that occurs in the region. We can thus see a relationship where the more confined a stream is, the lesser opportunity it has to adjust to the local geological setting, making the reach steeper and straighter with higher SL values and lower channel sinuosity values. Contrarily, when the streams are less confined and more able to shifting across the valley, they adjust to the local setting better, making the reach gentler and are more meandering in nature, returning a lower SL value and higher channel sinuosity value. Higher SL values are seen along segments of the Zanskar and western part of the Shyok (Fig. 17), that are situated within gorges. SL index values are the lowest along the central part of the Indus, near Leh, and around

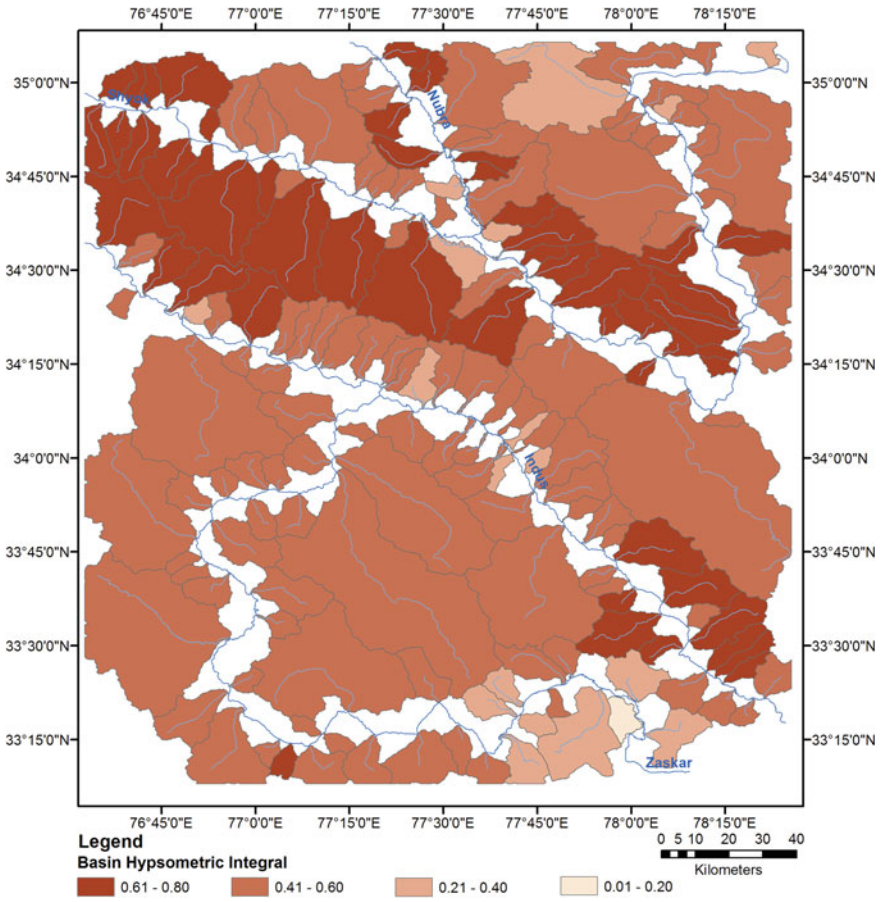

Fig. 14 Hypsometric Integrals for the mapped basins

the Nubra-Shyok confluence zone. It is exactly these channel segments that display a wide braided planform morphology, and thus the link between channel slope and form is apparent. The NSL values (Fig. 18) reflect the same picture. NSL values higher than 2.0 reflect steep courses while those higher than 10.0 are usually taken to reflect extremely steep courses, usually formed by uplift induced incision (Seeber and Gornitz 1983). Most segments here report values higher than 2.0 and the highest values are seen along the courses of the Shyok and Indus in the western part of the study area, where these rives transition into gorges after earlier occupying broader valley floors further to the east.

Examined individually, each of the main rivers' longitudinal profiles elicit pertinent information about its course. The initial part of the Indus's long profile (Fig. 19) shows a gently declining course before this translates into a steep fall in its latter half, dropping by about 1400 m over 350 km. The marked rise in the segment SL

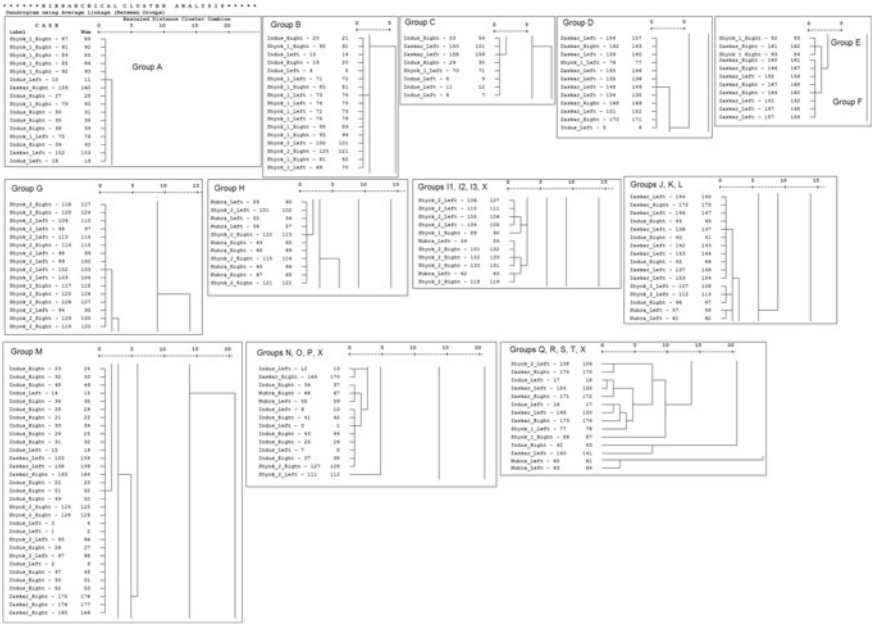

Fig. 15 Clusters formed on the basis of basin morphometric properties using a dendrogram. *Note* The figure presented here has been segmented out into smaller fragments due to its large size. The unbroken image can be supplied if required, upon request

values reflects this pertinently. Due to this steep course, the river profile shows little concavity in its course (the concavity value is 0.44). The mathematical curve that best fit its normalised profile was the exponential one ($R^2 = 0.975$). For the Zanskar (Fig. 20), the semi-log river long profile shows a number of sharp breaks. After an initial less steep segment, the curve falls sharply before again straightening out. This portion corresponds to the gentle middle section of the river, just after its confluence with its principal tributary, the Stod. Here the valley widens and a variety of depositional features have formed. Beyond this, the river enters a gorge that continues till its confluence with the Indus, and this is reflected in the steeply falling last portion of its long profile curve. The above changes are apparent in its markedly changing segment-wise SL values, being below 500 initially, then shooting up to four times that before dropping to the initial levels and then shooting up again. The exponential curve also best-fits the normalised long profile of this river. Of all the four studied rivers, the Zanskar's profile has developed possibly the greatest concavity (value is 0.54), due to its sharp fall in the upper reaches and then continued fall post the gentle middle segment. The semi-log plot of the Shyok's long profile (Fig. 21) also shows a number of breaks in the river's course. Its segment-wise SL index values show a steadily rising trend before dropping markedly between 350 and 450 km along its course. This portion corresponds to the broad valley that has formed at Diskit–Hunder and where the Nubra flows into it. Given the semi-confined nature of the river and

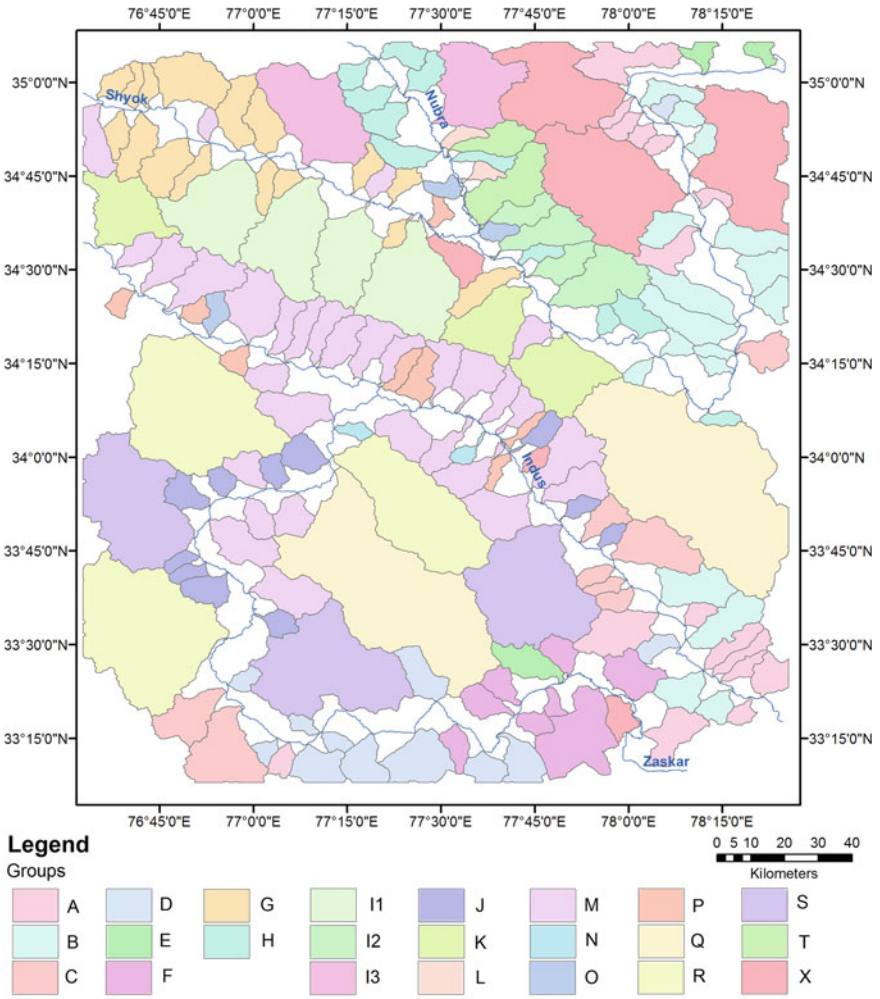

Fig. 16 Mapped basin clusters on basis of the devised dendrogram

the abundant supply of detritus from the surrounding terrain, an extensive braided channel planform has evolved herein (Fig. 25c). After this segment, the Shyok transitions into a gorge further to the west and this is reflected in its sharply rising SL index values. The exponential curve is again the best fit for its normalised profile form, while its constant drop has developed some measure of concavity in the profile (value is 0.34). The semi-log profile plot of the Nubra (Fig. 22) shows the least variations, compared to the other three rivers, due to its shorter length and the fact that it entirely occupies the Shyok Suture for the duration of its course. The river drops down at an almost constant rate and steepens slightly in its lowermost segments, just before its confluence with the Shyok. This is reflected in its segment-wise SL Index

Table 2 Basin groups ascertained through hierarchical cluster analysis based on basin morphological attributes

Basin group	No. of basins	Remarks
A	16	Scattered basins in the Zaskar region, mostly concentrated around its headwater reaches, amidst heavily dissected hill ranges
B	17	Basins that are mostly clustered along the upper section of the Shyok, just prior to and after its great bend and which drain both flanks of it
C	8	Basins that cluster in the upper sections of the Zaskar and around the eastern section of the Indus' course
D	12	These basins cluster around the upper to middle course of the Zanskar, primarily draining its right flank
E	3	These basins are scattered around the headwater reaches of the Zanskar and Shyok
F	8	Located within the medium to highly dissected structural hills around the upper reaches of the Zanskar
G	16	Clustered around the steepest segments of the Shyok in the westernmost part of its course in the study area, draining down both its flanks
H	11	Basins mostly clustered around the upper course of the Nubra, on its right flank
I1	4	Larger basins that arise on the northern flank of the Karakoram and drain into the Nubra on its right flank
I2	4	Smaller and elongated basins that arise in the Karakorams and drain the left flank of the Nubra and the Shyok's right flank just before they meet
I3	2	These are larger sized basins that drain either into the upper section of the Nubra or the steep western segments of the Shyok
J	11	This is a group of some of the smallest sub-basins, that are often located on the extensive piedmonts, between the mouths or larger sub-basins. The mostly drain into the Zanskar, in its central section, where its valley has widened considerably
K	3	Medium sized basins that drain into the Shyok just after its sharp turn towards the northwest and into the steeper western segment of the Indus
L	2	Quite small sub-basins that are present between the lower sections of larger basins and drain the left flank of the Nubra into it
M	31	The Group with the largest number of sub-basins, almost all of which are of smaller dimensions, arise from the southern flank of the Ladakh Range and flow into the left flank of the Indus. Some of these arise from the opposite flank too, particularly over the extensively dissected northern flank of the Zaskar Range and the substantial pediment surfaces that have formed opposite Leh and Choglamsar and near Stok. These basins are essentially steep mountain flank originating small parallel basins

(continued)

Table 2 (continued)

Basin group	No. of basins	Remarks
N	2	Very small, narrow basins lying between larger members, that drain the southern face of the Zanskar Range into the Indus and Zanskar rivers
O	3	Quite small, elongated sub-basins situated between larger members and mostly flowing into the Nubra-Shyok near their confluence zone
P	8	Small confined basins that lie on either side of the Indus Thrust and Suture Zone and drain into this river
Q	2	This group denotes the largest sub-basins in the study area, one of which drains into the Zanskar and the other into the Indus in its eastern section
R	3	This group contains the next largest sub-basins in terms of size, after Group Q and all of these drain into the Zanskar, on both its left and right flanks
S	3	Medium to large sized sub-basins situated in the dissected hill ranges of the Zaskar Basin and draining into it or into the Indus towards the north
T	2	Small group that is present by the Nubra's left flank
X	6	Singular basins, without any group members. These are scattered across the study area

variations and the near-constant drop has made the linear trendline the best-fit for its normalised long profile curve. The concavity value is low at 0.39.

Thus, the two more southern rivers, the Indus and the Zanskar, have higher concavity values, indicating a possibly greater ongoing erosion process. Situated within the Karakoram, the Shyok and Nubra have slightly lower concavities, indicating possibly a greater incidence of uplift that has kept channel segments steeper. Comparison of the best fit curves show that in three cases the logarithmic trendline was the best fit while the linear trendline was the best fit in one case. However, in each case, the R^2 values of the logarithmic and linear trendlines were quite close to each other. This is indicative of the coarse bedload that characterise these rivers and cause braiding to occur in certain stretches, while also hinting at a yet to be achieved equilibrium condition for these streams, possibly due to the ongoing tectonic movements that perturb the channel. However, these conclusions are mere surmises and no generalisations should be drawn on the basis of a single parameter or index-based evaluation, without ancillary data and field information. What is undeniable, however, is the role that the regional geological structures and tectonics have had in influencing the channel morphologies and alignments. This is examined in more detail in the next section.

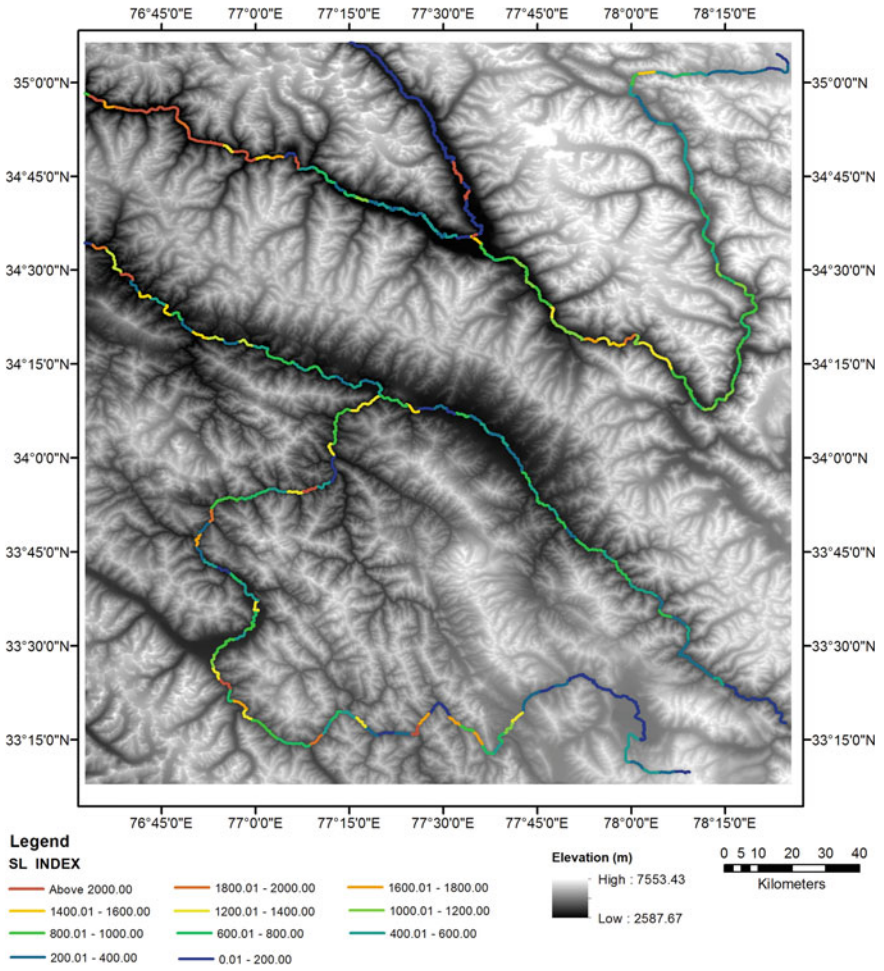

Fig. 17 Mapped SL Index values for the principal drainage lines

5.4 Principal Drainage Lines, Valley Form and Channel Morphology

The strong controls exercised by the various mountain fronts all over the Himalayas is evident from the courses of the rivers that flow through it. Such rivers are generally characterised by straightened courses, v-shaped valleys, asymmetric and oval-shaped watersheds and sharp knee bend turns of seasonal rivulets and incised meanders, as channels adjust to the surface they are flowing over and these are directly related to the lithology and geology of the area. The channels carve out their landforms and vary diversely from an alluvial channel to a bedrock channel. O'Brien et al. (2019) defined channel confinement as the percentage of the length of a channel margin that

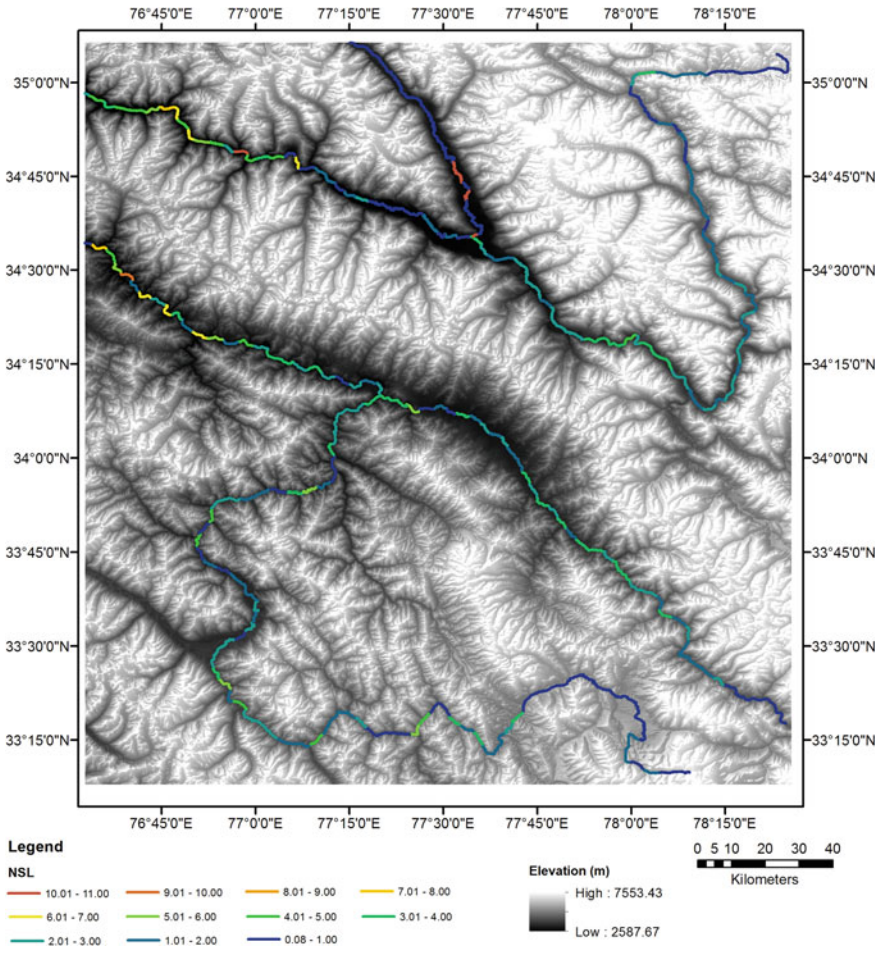

Fig. 18 Mapped NSL values for the principal drainage lines

abuts a confining margin on either bank. Channel confinement gives us an idea as to what degree the channel has the freedom to move and adjust to the rocks beneath it. Channel slope and scale is often used to determine the level of adjustment of a river but in most cases, the simplest way is by comparing the channel width to the valley width. (O'Brien et al. 2019). When the channel width is equal to the valley width, it means that the channel is flowing across the entire valley with no space for the stream to move and hence adjust to the local setting. Such channels are generally geometrically straighter with little to no bends and both flanks of the channel are in contact with the valley edge. In other cases, when the river is meandering within the valley, the channel width is always lesser than that of the valley width allowing the stream to roll over from one edge of the valley to another and giving the stream enough space to adjust to the local setting. In such cases, either end of the stream

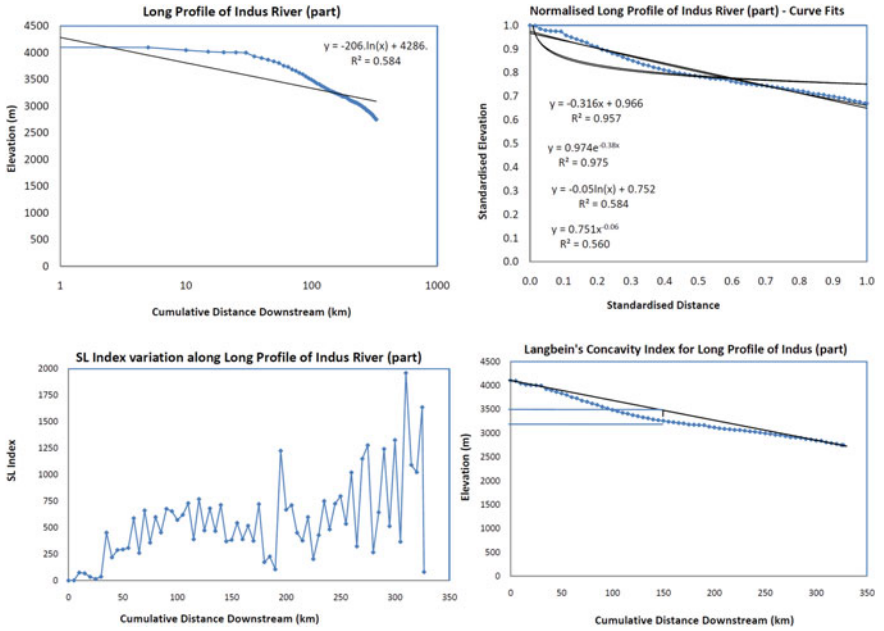

Fig. 19 Long profile plot and curve-fitting for the River Indus, along with reach-wise SL Index variations and computation of the Langbein's concavity parameter

might be in contact with the valley edge or may have both ends of the stream freely flowing within the valley. These channels are generally not straight and can have considerable sinuosity to them.

The above structural control induced channel confinement aspect is seen to markedly influence the valley form, channel morphology and formed geomorphic units in the study area along its principal rivers. Here, the main valleys stand out as broad lower elevation ribbons, especially the confluence zone of the Nubra and Shyok rivers and the Indus at Leh, and have wider river corridors. The Indus flows southeast to northwest across the central part of the area and is joined on its left flank by the Zanskar river near Nimo Peak. The gradual widening of the Indus valley can be observed from its narrow linear form towards the east and subsequent increase in width in the central portion alongside the settlements of Leh, Stok and Choglamsar, just before it is met by the Zanskar and then the Yappola (Fig. 23). Beyond this, the valley width is maintained almost uniformly, though to a lesser extent than was seen in the central portion. This wide central portion is characterised by extensive piedmont surfaces (Fig. 26c), valley margin alluvial fans, high fan-talus (cf. Wadia 1919) and scree deposits and the braided character of the main channel (Fig. 24a, Fig. 25a–d). The Zanskar forms by the meeting of the Tsarap-Lungnak and Stod rivers, at which point its valley widens considerably to the greatest extent along its course, in the south-western portion of the study area. This short wide section of the Zanskar valley contains the greatest diversity of geomorphic forms along its course,

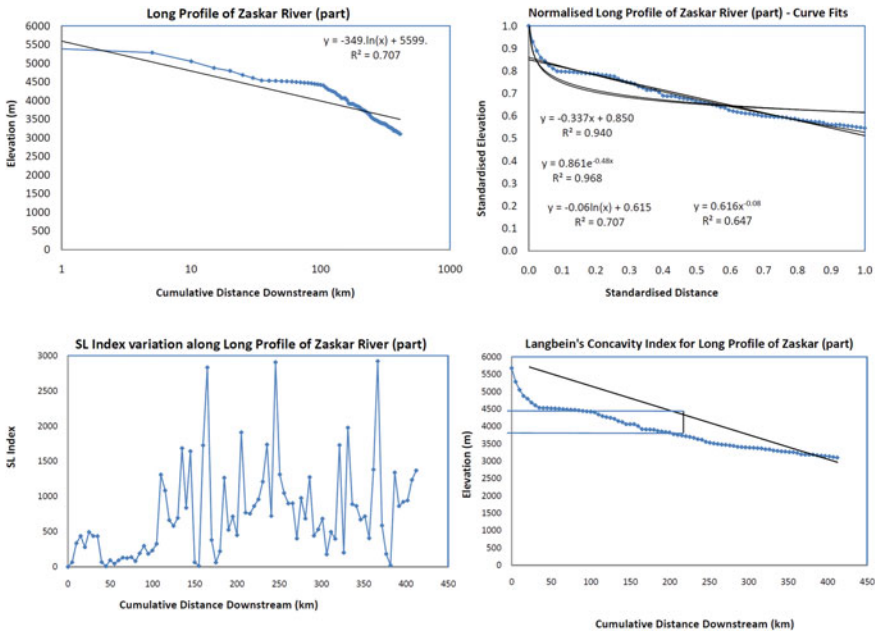

Fig. 20 Long profile plot and curve-fitting for the River Zanskar, along with reach-wise SL Index variations and computation of the Langbein's concavity parameter

being occupied by several small alluvial fans, large mid-channels bars that cause extensive braiding in this stretch, talus deposits and abutting dissected hill ranges (Fig. 24c). After this, the river flows through a gorge for almost the entire extent of its remaining course before debouching into the Indus (Fig. 24b). The Nubra arises from the Siachen Glacier which is just to the north of the demarcated study area. It flows through a broad glacial valley and is a markedly braided river for its entire course (Fig. 23). Its valley sides are occupied by a number of alluvial fans formed by the steeply dropping streams along either flank. These alluvial fans have been further incised due to repeated regional uplift and thus are flanked by paired terraces along their margins, formed of past deposits. Often the surface of the present fan is occupied by small settlements (Fig. 25b and c). A considerable length of the Shyok is present in the study area and its course most aptly depicts the strong structural control exerted by the parallel Trans-Himalayan ranges and their associated suture zones and fault lines. The Shyok enters the study area at its upper right corner, flows due south in a narrow valley, before taking a sharp but pronounced bend to turn all the way towards the northwest, by an angle of >90° (Fig. 24d). After this turn, the river is flanked by extensive piedmont slopes as the valley widens out manifold times towards its confluence with the Nubra.

The confluence zone of the Nubra and Shyok rivers is the largest lower elevation zone in the entire region along with the Leh town piedmont surface and is discernable by its valley widths of around 2.5–3.0 km (Fig. 24e). This wide floodplain represents

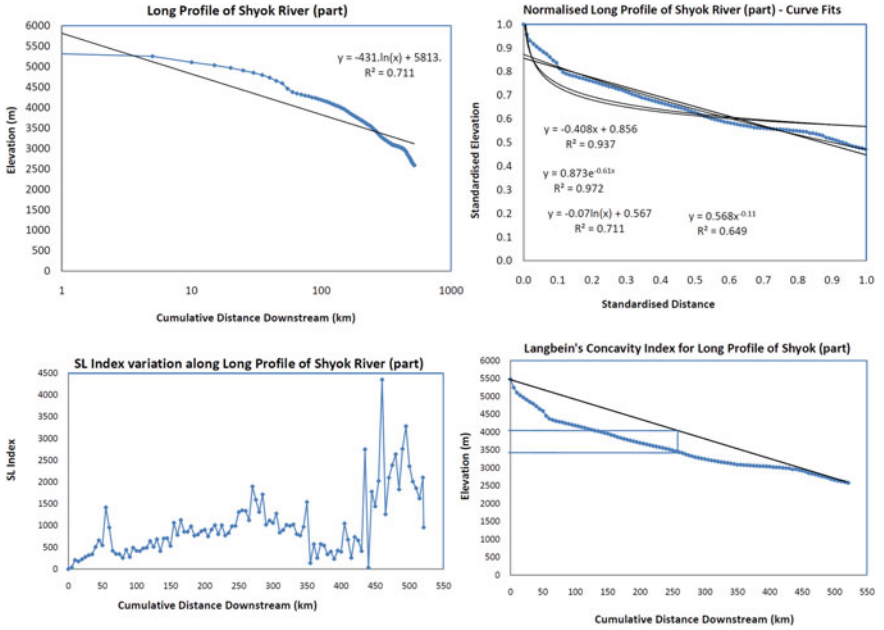

Fig. 21 Long profile plot and curve-fitting for the River Shyok, along with reach-wise SL Index variations and computation of the Langbein's concavity parameter

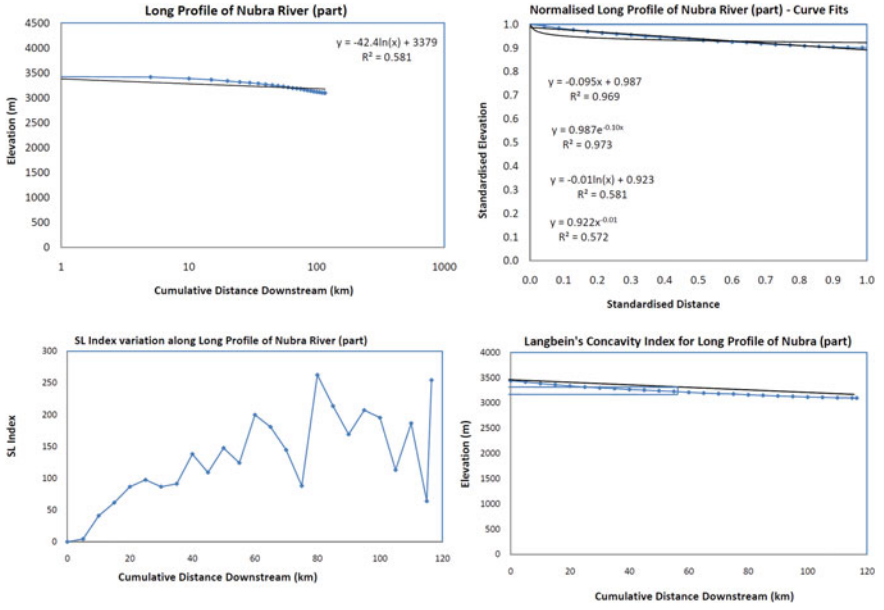

Fig. 22 Long profile plot and curve-fitting for the River Nubra, along with reach-wise SL Index variations and computation of the Langbein's concavity parameter

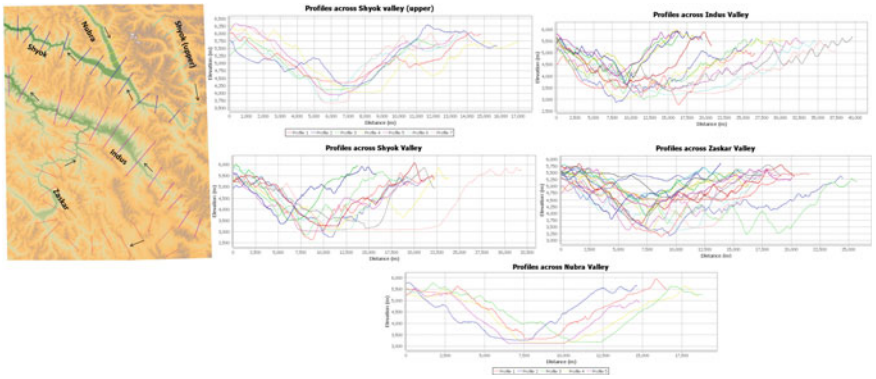

Fig. 23 Valley cross-sections across the principal rivers

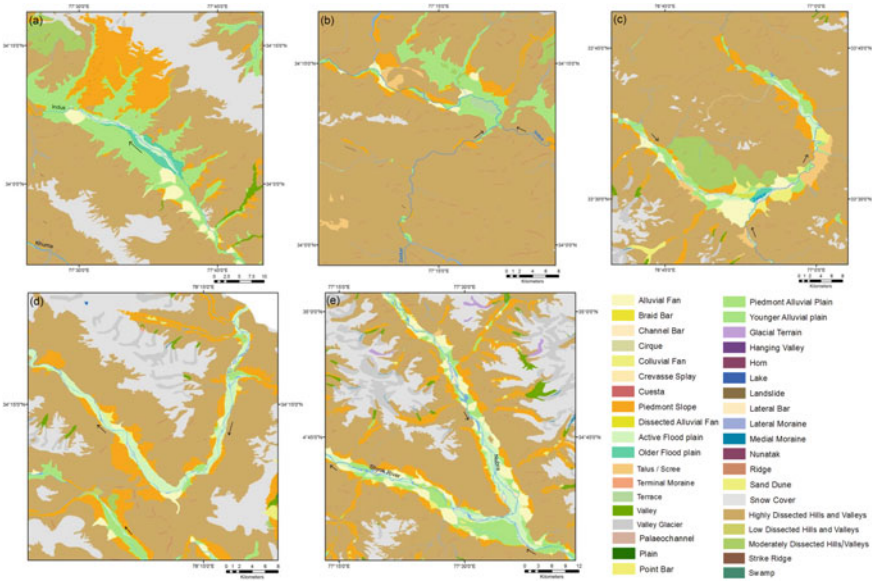

Fig. 24 Different geomorphic units present in the landscape and associated channel morphology in select reaches of the principal rivers. **a** Central part of the Indus' course around Leh. **b** Confluence of the Zanskar with Indus. **c** Confluence of the Stod and Zanskar, with resultant wide valley segment with diverse geomorphic forms. **d** The great bend of the Shyok, turning from going towards due south to towards the northwest, after occupying the Karakoram Fault. **e** The confluence zone of the Nubra and Shyok rivers in an obtuse barbed meeting and the resultant wide valley floor formation

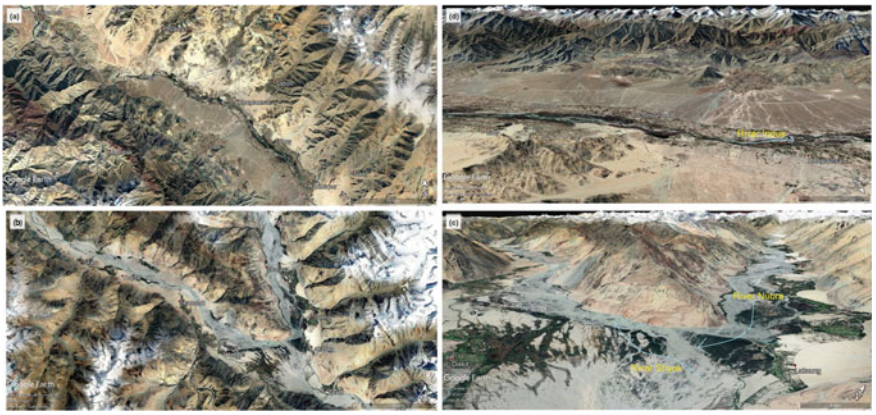

Fig. 25 Google earth views of the channel morphology and adjacent valley geomorphic features in plan view and in tilted 3D view—**a** and **d** for the central part of the Indus valley near Leh, Stok and Choglamsar, with extensive pediments on the southern flank and valley fills and alluvial fans on the northern side wherein banded and inclined rock formations are also discernable along the dissected triangular scarp facets; **b** and **c** the obtuse/barded confluence zone of the Nubra and Shyok rivers near the village of Diskit, with the two valleys being separated by the intervening Great Karakoram Range

the obtuse and barbed drainage confluence of these two rivers, with the Nubra flowing in almost a completely opposite direction to the Shyok, as both of these rivers occupy their respective fault zones (Fig. 25b and c). Their confluence zone around the villages of Diskit and Hunder is also unique in having some high-altitude wetlands and barchanoid sand dunes that have developed in the broad space created by these two rivers via sediment infilling of the Karakoram fault and Shyok Sutures (Fig. 26n). The broad nature of the Shyok valley (Fig. 26o) is retained for some duration after this confluence as the river occupies a central position and extensively braids over the rest of its course here before it transitions into a narrower channel and then moves into a gorge further west.

The highly braided nature of some of these main channel segments is typically what happens in the Himalayan region when adequate valley width is available, usually due to tectonic and warping processes and then infilling of these zones by laid down deposits and the marked sediment supply from hillslopes and river discharge variability (Rajbanshi et al. 2022). It also points to the marked denudation that occurs throughout this region, not only by fluvial processes but also by substantial physical weathering due to the great extremities of the weather elements in daily and seasonal timescales and the intense insolation received here, as pointed out before. The exposed and bare hillslopes, which are almost entirely devoid of any vegetation, often have thick weathered angular rock fragments at their base. Adding to this is the sheetflow and rill erosion that occurs along these slopes. Thus large fan-talus forms are seen to occupy the valley margin areas and their materials are gradually worked into the main channels by tributaries. The other source of sediment supply comes

Fig. 26 Field photographs of the Ladakh region and the study area. **a** Sharp anticlines in the Zanskar Range. **b** Large fan-talus deposits near Dras. **c** Extensive bare pediment surface along the southern flank of the Indus opposite Leh. **d** Re-incised alluvial fan surface and fan front margin near Dras indicating possible latter day uplift after initial deposition. **e** Glacial valley near Khardung La. **f** Meeting of two former glacial valleys that then form a piedmont zone near Leh. **g** Moraine near Khardung village that has been partly levelled and used for cultivation. **h** Apparent recumbent fold in the Zanskar range. **i** Moonland at Lamayuru, possibly indicating a former lake that has been uplifted, drained and heavily dissected. **j** Possible white salina surface, resulting from evaporation of a playa lake, along the Muree Plains within the Zanskar Range. **k** Possible homoclinal rock attitude along the Zanskar Range opposite Choglamsar indicating the great uplift and tilting that has occurred. **l** Folded and vertical rock alignments in the Zanskar Range of many hues. **m** Looking across the Shyok valley at Hunder village, with the seasonal wetlands in the foreground and the dissected surface of the a portion of the Great Karakorams in the background. **n** High altitude barchans in the foreground that have formed along the Shyok plains near Hunder village, with the braided Shyok River in the background. **o** The extensive braided nature of the Shyok River, which is occupying the Karakoram Fault and the wide valley floor across which it traverses. **p** A tributary arising from the Great Karakoram range confluences with the Shyok River, having cut down through its past deposits that are present as paired terraces on either flank of its present lower vegetated alluvial fan surface. *Note* All the photographs have been taken by the first author

from reworked past glacial deposits, with a number of moraines present in this area (e.g. the moraine deposits at Khardung village- Fig. 26g). Past and ongoing uplift can also result in hydrological changes, by raising lake beds, leading to their dissection (e.g. what has occurred in the Moonlands of Lamayuru (Kotlia et al. 1997)—Fig. 26i). Conversely, the basins formed within the uplifted ranges can also house extensive piedmont zones and low-lying playas (Fig. 26j) where local runoff can accumulate

and form lakes, which usually dry up and leave behind salinas, while along the main channels like the Shyok and Indus, particularly where their tributaries flow in, local seasonal grasslands/wetlands also arise that are usually used as pasturelands.

6 Conclusions

This paper has tried to briefly bring out the notable lithologic and structural elements of a part of the Ladakh region and relate them with the enumerated terrain parameters and ambient river character. The high mountain landscape and the associated tectonic and structural elements have abetted the formation of very confined to partly unconfined river channels. While the main rivers have some wider valley segments, occupied by extensive channel braids, the tributaries are incised and of bedrock character. Both erosional and depositional forms are seen, with the former being more extensive and manifesting as numerous dissected ridges of varying degrees and substantial pediment surfaces. The depositional features are more localised, whether they be in-channel bars or channel adjacent alluvial fans. The extent to which such depositional elements have formed largely rests on the available valley floor space, which is in turn dependent on the compressional/extensional and shearing movements that have occurred herein. In-filling of such available spaces by unconsolidated deposits borne by the principal rivers and supplied by their many tributaries have enabled the formation of sustained flatter surfaces in some locations, which serve as settlement points (e.g. on valley floors or lower fan surfaces). The alignments of almost all streams are controlled by the underlying sutures, faults and their associated thrust elements. Greater insight into the evolutionary history of the drainage and its linkages with the ambient past and present tectonic elements can be better ascertained through detailed sediment/rock dating, reach-scale denudation rates and facies analysis of the deposited sediment profiles along the main and tributary channels.

Acknowledgements The authors are grateful to Mr. Rajarshi Dasgupta of the Department of Geography, East Calcutta Girls' College, Kolkata and Dr. Somasis Sengupta of the Department of Geography, The University of Burdwan, Barddhaman, for their inputs regarding the paper.

References

Allamano A, Claps P, Laio F (2009) Global warming increases flood risk in mountainous areas. Geophys Res Lett 36:L24404. https://doi.org/10.1029/2009GL041395

Ambili V, Narayana AC (2014) Tectonic effects on the longitudinal profiles of the Chaliyar River and its tributaries, southwest India. Geomorphology 217:37–47

Anand AK, Pradhan SP (2019) Assessment of active tectonics from geomorphic indices and morphometric parameters in part of the Ganga basin. J Mt Sci 16:1943–1961. https://doi.org/10.1007/s11629-018-5172-2

Ashrit R (2010) Investigating the Leh 'Cloudburst'. National Centre for Medium Range Weather Forecasting, Ministry of Earth Sciences, Government of India. http://www.ncmrwf.gov.in/Cloudburst_Investigation_Report.pdf]. Accessed 26 April 2016

Banerji D, Patel PP (2019) Morphological aspects of the Bakreshwar River Corridor, West Bengal, India. In: Das B, Ghosh S, Islam A (eds) Advances in micro geomorphology of lower Ganga Basin—Part I: Fluvial geomorphology. Springer International Publishing, Cham, pp 155–189. https://doi.org/10.1007/978-3-319-90427-6_9

Barnett TP, Adam JC, Lettenmaier DP (2005) Potential impacts of a warming climate on water availability in snow-dominated regions. Nature 438:303–309

Benn DI, Owen LA (1998) The role of Indian summer monsoon and the mid-latitude westerlies in Himalayan glaciation: review and speculative discussion. J Geol Soc London 155:353–363

Bhan SC, Devrani AK, Sinha V (2015) An analysis of monthly rainfall and the meteorological conditions associated with cloudburst over the dry region of Leh (Ladakh), India. Mausam 66:107–122

Bharadwaj H, Singh AP, Malhotra MS (1973) Body comparison of the high-altitude natives of Ladakh: a comparison with sea-level residents. Hum Biol 45:423–434

Bhatt CM, Litoria PK, Sharma PK (2008) Geomorphic signatures of active tectonics in Bist Doab interfluvial tract of Punjab, NW India. J Indian Soc Remote Sens 36(4):361–373

Bhutiyani MK (2014) The Siachen Glacier: the second longest glacier outside the polar regions. In: Kale VS (ed) Landscapes and Landforms of India. Springer, Dordrecht, pp 105–113

Bhutiyani MK, Kale VS, Pawar NJ (2010) Climate change and the precipitation variations in the northwestern Himalaya: 1866 to 2006. Int J Climatol 30:535–548

Bookhagen B, Burbank DW (2006) Topography, relief and TRMM-derived rainfall variations along the Himalaya. Geophys Res Lett 33:L08405. https://doi.org/10.1029/2006GL026037

Brocklehurst SH (2010) Tectonics and geomorphology. Prog Phys Geogr 34:357–383. https://doi.org/10.1177/0309133309360632

Bull WB (2007) Tectonic geomorphology of mountains: a new approach to paleoseismology. Wiley-Blackwell, Oxford

Bull WB, McFadden L (1977) Tectonic geomorphology north and south of the Garlock fault, California. In: Doehring DO (eds) Geomorphology in arid regions. Proceedings of the 8th Annual Geomorphology Symposium), State University of New York, Binghamton, pp 115–138

Bull WB (1977) Tectonic geomorphology of the Mojave Desert. U.S. Geological Survey Contract Report 14-08-001-G-394. Office of Earthquakes, Volcanoes, and Engineering, Menlo Park, California

Bull WB (1978) Geomorphic tectonic classes of the south front of the San Gabriel Mountain, California. U.S. Geological Survey Contract Report 14-08-001-G-394. Office of Earthquakes, Volcanoes, and Engineering, Menlo Park, California

Burbank DW, Anderson RS (2011) Tectonic geomorphology. Wiley, New Jersey

Burbank DW, Leland J, Fielding E, Anderson RS, Brozovic N, Reid MR, Duncan C (1996) Bedrock incision, rock uplift and threshold hillslopes in the northwestern Himalayas. Nature 379:505–510

Castillo M, Munoz-Salinas E, Ferrari L (2014) Response of a landscape to active tectonics using channel steepness indices (k_{sn}) and OSL: a case study from the Jaliso block, western Mexico. Geomorphology 221:204–214. https://doi.org/10.1016/j.geomorph.2014.06.017

Church M, Ryder JM (1972) Paraglacial sedimentation: a consideration of fluvial processes conditioned by glaciation. Geol Soc Am Bull 83:3059–3072

Clift PD (2002) A brief history of the Indus River. In: Clift PD, Kroon D, Gaedicke C, Craig J (eds) The tectonic and climatic evolution of the Arabian Sea region, vol 195. Geological Society of London Special Publications. Geological Society of London, London, pp 237–258

Cox RT (1994) Analysis of drainage-basin symmetry as a rapid technique to identify areas of possible Quaternary tilt-block tectonics: an example from the Mississippi Embayment. Geol Soc Am Bull 106(5):571–581. https://doi.org/10.1130/00167606(1994)1062.3.CO;2

Cunningham A (1854) Ladak, physical, historical and statistical. W.H. Allen & Company, London

Dar RA, Chandra R, Romshoo SA (2013) Morphotectonic and lithostratigraphic analysis of intermontane Karewa basin of Kashmir Himalayas, India. J Mt Sci 10:1–15. https://doi.org/10.1007/s11629-013-2494-y

Das S, Patel PP, Sengupta S (2016) Evaluation of different digital elevation models for analyzing drainage morphometric parameters in a mountainous terrain: a case study of the Supin. Upper Tons Basin, Indian Himalayas. SpringerPlus, vol 5, p 1544. https://doi.org/10.1186/s40064-016-3207-0

Doornkamp JC (1986) Geomorphological approaches to the study of neotectonics. J Geol Soc 143:335–342. https://doi.org/10.1144/gsjgs.143.2.0335

Dortch JM, Owen LA, Caffee MW (2010) Quaternary glaciation in the Nubra and Shyok valley confluence, northernmost Ladakh, India. Quatern Res 74:132–144

Dortch JM, Owen LA, Caffee MW (2013) Timing and climatic drivers for glaciation across semi-arid western Himalaya-Tibetan orogen. Quatern Sci Rev 78:188–208

Drew F (1875) The Jummoo and Kashmir territories: a geographical account. Edward Stanford, London

Duncan C, Masek J, Fielding E (2003) How steep are the Himalaya? Characteristics and implications of alongstrike topographic variations. Geology 31:75–78

England P, Molnar P (1990) Surface uplift, uplift of rocks, and exhumation of rocks. Geology 18:1173–1177

Evans IS, Hengl T, Gorsevski P (2009) Applications in geomorphology. In: Hengl T, Reuter HI (eds) Geomorphometry: concepts, software, applications. Developments in soil science, vol 33, pp 497–525. https://doi.org/10.1016/S0166-2481(08)00022-6

Fielding EJ (1996) Tibet uplift and erosion. Tectonophysics 260:55–84

Florinsky IV (2017) An illustrated introduction to general geomorphometry. Prog Phys Geogr 41:723–752

Ganjoo RK, Koul MN, Bahuguna IM, Ajai (2014) The complex phenomenon of glaciers of Nubra Valley, Karakorum (Ladakh), India. Nat Sci 6:733–740

Gansser A (1964) Geology of the Himalaya. Wiley-Interscience, London

Gruber S, Peckham S (2009) Land surface parameters and objects in hydrology. In: Hengl T, Reuter HI (eds) Geomorphometry: concepts, software, applications. Developments in soil science, vol 33, pp 171–194. https://doi.org/10.1016/S0166-2481(08)00007-X

Guha S, Patel PP (2017) Evidence of topographic disequilibrium in the Subarnarekha River Basin, India: a digital elevation model based analysis. J Earth Syst Sci 126:106. https://doi.org/10.1007/s12040-017-0884-1

Hack JT (1973) Stream profile analysis and stream-gradient index. J Res US Geol Surv 1:421–429

Hare PW, Gardner TW (1985) Geomorphic indicators of vertical neotectonism along converging plate margins, Nicoya Peninsula, Costa Rica. In: Morisawa M, Hack JT (eds) Tectonic geomorphology. Proceedings of the 15th Annual Binghamton Geomorphology Symposium. Allen and Unwin, Boston, MA, pp 123–134

Harlin JM (1978) Statistical moments of the hypsometric curve and its density function. Int J Assoc Math Geol 10:59–72

Hedrick KA, Seong YB, Owen LA, Caffee MW, Dietsch C (2011) Towards defining the transition in style and timing of Quaternary glaciation between the monsoon-influenced Greater Himalaya and the semi-arid Transhimalaya of northern India. Quatern Int 236:21–33

Hobley DEJ, Sinclair HD, Mudd SM (2012) Reconstruction of a major storm event from its geomorphic signature: the Ladakh floods, 6 August 2010. Geology 40:483–486

Imsong W, Bhattacharya F, Mishra RL, Phukan S (2017) Geomorphic evidence of late Quaternary displacement of the Karakoram Fault in Nubra and Shyok valleys, Ladakh Himalaya.Curr Sci 2295–2305

Jacobson A (2000) Solar energy measurements for Ladakh, India. In: Banerjee R, Nayak JK, Fernandes BG (eds) Renewable energy technology for the new millennium, Proceedings of the 24th national renewable energy convention. Allied Publishers Limited, New Delhi

Jamieson SSR, Sinclair HD, Kirstein LA, Purves RS (2004) Tectonic forcing of longitudinal valleys in the Himalaya: morphological analysis of the Ladakh batholith, north India. Geomorphology 58:49–65

Juyal N (2010) Cloud burst-trigged debris flow around Leh. Curr Sci 99:1166–1167

Juyal N (2014) Ladakh: the high-altitude Indian cold desert. In: Kale VS (ed) Landscapes and Landforms of India. Springer, Dordrecht, pp 115–124

Kale VS, Achyuthan H, Sengupta S (2010) Reconstruction of late quaternary fluvio-sedimentary response of Kaveri and Palar Rivers: based on Chronostratigraphy, Digital geomorphometry and remote sensing analysis. University of Pune, Pune

Keller EA, Pinter N (2002) Active tectonics: earthquakes, uplift and landscape, 2nd edn. Prentice Hall, Upper Saddle River, New Jersey

Knighton D (1998) Fluvial forms and processes: a new perspective. Routledge

Kotlia BS, Shukla UK, Bhalla MS, Mathur PD, Pant CC (1997) Quaternary fluvio-lacustrine deposits of the Lamayuru Basin, Ladakh Himalaya: preliminary multidisciplinary investigations. Geol Mag 134(6):807–812

Kumar A, Srivastava P (2018) Landscape of the Indus River. In: Singh D (ed) The Indian Rivers. Springer, pp 47–59

Kumar MS, Shekhar MS, Rama Krishna SSVS, Bhutiyani MR, Ganju A (2012) Numerical simulation of cloud burst event on August 05, 2010, over Leh using WRF mesoscale model. Nat Hazards 62:1261–1271

Langbein WB (1964) Profiles of rivers of uniform discharge. US Geol Surv Prof Pap 501B:119–122

Lee CS, Tsai LL (2010) A quantitative analysis for geomorphic indices of longitudinal river profile: a case study of the Choushui River, Central Taiwan. Environ Earth Sci 59:1549–1558

Lin Z, Oguchi T (2004) Drainage density, slope angle, and relative basin position in Japanese bare lands from high-resolution DEMs. Geomorphology 63(3–4):159–173

Lin Z, Oguchi T (2006) DEM analysis on longitudinal and transverse profiles of steep mountainous watersheds. Geomorphology 78:77–89

Lohan SK, Sharma S (2012) Present status of renewable energy resources in Jammu & Kashmir state of India. Renew Sustain Energy Rev 16:3251–3258

Mahmood SA, Gloaguen R (2012) Appraisal of active tectonics in Hindu Kush: insights from DEM derived geomorphic indices and drainage analysis. Geosci Front 3:407–428. https://doi.org/10.1016/j.gsf.2011.12.002

Munack H, Korup O, Resentini A, Limonta A, Garsanti E, Blothe JH, Scherler D, Wittman H, Kubik PW (2014) Postglacial denudation of western Tibetan plateau margin outspaced by long-term exhumation. Bull Geol Soc America 126:1580–1594. https://doi.org/10.1130/B30979.1

Nag SK, Chakraborty S (2003) Influence of rock types and structures in the development of drainage network in hard rock area. J Indian Soc Remote Sens 31:25–35

Nag D, Phartiyal B, Joshi M (2021) Late Quaternary tectono-geomorphic forcing vis-a-vis topographic evolution of Indus catchment, Ladakh. India. Catena 199:105103. https://doi.org/10.1016/j.catena.2020.105103

Nagar DP, Ahmed Z (2007) Biological spectrum of Nubra Valley (Ladakh). Indian J Forest 30:479–481

O'Brien GR, Wheaton JM, Fryirs K, Macfarlane WW, Brierley G, Whitehead K, Gilbert J, Volk C (2019) Mapping valley bottom confinement at the network scale. Earth Surf Proc Land 44(9):1828–1845

Oguchi T (1997) Drainage density and relative relief in humid steep mountains with frequent slope failure. Earth Surf Proc Land 22:107–120. https://doi.org/10.1002/(SICI)1096-9837(199702)22:2%3c107::AID-ESP680%3e3.0.CO;2-U

Olaya V (2009) Basic land-surface parameters. In: Hengl T, Reuter HI (eds) Geomorphometry: concepts, software, applications. Developments in soil science, vol 33, pp 141–69. https://doi.org/10.1016/S0166-2481(08)00006-8

Osmaston H (1994) The geology, geomorphology and Quaternary history of Zangskar. In: Crook J, Osmaston H (eds) Himalayan Buddhist villages: environment, resources, society and religious life in Zangskar, Ladakh. University of Bristol Press, Bristol, pp 1–36

Owen LA (2014) Himalayan landscapes of India. In: Kale VS (ed) Landscapes and landforms of India. Springer, Dordrecht, pp 41–52

Owen LA, Dortch JM (2014) Nature and timing of Quaternary glaciation in the Himalayan-Tibetan orogen. Quatern Sci Rev 88:14–54

Owen LA (2011) Quaternary glaciation of northern India. In: Elhers J, Gibbard P, Hughes PD (eds) Quaternary glaciations: extent and chronology: a closer look. Developments in quaternary science, vol 15. Elsevier, Amsterdam, pp 929–942

Palmer TN, Rälsänen J (2002) Quantifying the risk of extreme seasonal precipitation events in a changing climate. Nature 415:512–514

Patel PP (2012) An exploratory geomorphological analysis using modern techniques for sustainable development of the Dulung river basin. Unpublished Ph.D. thesis, University of Calcutta, Kolkata. https://sg.inflibnet.ac.in/handle/10603/156681

Patel PP (2013) GIS techniques for landscape analysis—case study of the Chel River Basin, West Bengal. In:Proceedings of state level seminar on geographical methods in the appraisal of landscape, held at Department of Geography, Dum Dum Motijheel Mahavidyalaya, Kolkata, 20 March 2012, pp 1–14

Patel PP, Sarkar A (2007) Hypsometric analysis of the Dulung N. Basin and its sub-basins. Geograph Rev India 69(4):409–422

Patel PP, Sarkar A (2009) Application of SRTM data in evaluating the morphometric attributes: a case study of the Dulung River Basin. Pract Geographer 13(2):249–265

Patel PP, Sarkar A (2010) Terrain characterization using SRTM data. J Indian Soc Remote Sens 38(1):11–24. https://doi.org/10.1007/s12524-010-0008-8

Patel PP, Dasgupta R, Chanda S, Mondal S (2021) An investigation into longitudinal forms of gullies within the "Grand Canyon" of Bengal, Eastern India. Trans GIS 25(5):2501–2528. https://doi.org/10.1111/tgis.12828

Perez-Pena JV, Azanon JM, Azor A (2008) CalHypso: an ArcGIS extension to calculate hypsometric curves and their statistical moments. Comput Geosci 35:1214–1223

Phartiyal B, Kothyari GC (2012) Impact of neotectonicson drainage network evolution reconstructed from morphometric indices: case study from NW Indian Himalaya. Zeitschrift Fur Geomorphologie 56:121–140. https://doi.org/10.1127/0372-8854/2011/0059

Phartiyal B, Sharma A, Upadhyay R, Sinha AK (2005) Quaternary geology, tectonics and distribution of palaeo-and present fluvio/glacio lacustrine deposits in Ladakh, NW Indian Himalaya—a study based on field observations. Geomorphology 65(3–4):241–256

Pike RJ (2000) Geomorphometry: diversity in quantitative surface analysis. Prog Phys Geogr 24:1–20

Pike RJ, Evans IS, Hengl T (2009) Geomorphometry: a brief guide. In: Hengl T, Reuter HI (eds) Geomorphometry: concepts, software, applications. Developments in soil science, vol 33, pp 3–30. https://doi.org/10.1016/S0166-2481(08)00001-9

Prerna R, Pandey DK, Mahender K (2018) Longitudinal profiling and elevation-relief analysis of the Indus. Arab J Geosci 11:343. https://doi.org/10.1007/s12517-018-3657-5

Radaideh OMA, Mosar J (2019) Tectonic controls on fluvial landscapes and drainage development in the westernmost part of Switzerland: insights from DEM-derived geomorphic indices. Tectonophysics 768:228179

Rajbanshi J, Das S, Patel PP (2022) Planform changes and alterations of longitudinal connectivity caused by the 2019 flood event on the braided Brahmaputra River in Assam, India. Geomorphol 403:108174. https://doi.org/10.1016/j.geomorph.2022.108174

Ramachandra TV, Jain R, Krishnadas G (2011) Hotspots of solar potential in India. Renew Sustain Energy Rev 15:3178–3186

Ramirez-Herrera MT (1998) Geomorphic assessment of active tectonics in the Acambay graben, Mexican volcanic belt. Earth Surf Proc Land 23:317–332

Rasmussen KL, House RA Jr (2012) A flash-flooding storm at the steep edge of high terrain. Bull Am Meteor Soc 93:1713–1724
Remondo J, Oguchi T (2009) Editorial- GIS and SDA applications in geomorphology. Geomorphology 111:1–3. https://doi.org/10.1016/j.geomorph.2009.04.015
Robl J, Stuwe K, Hergarten S (2008) Channel profiles around Himalayan river anticlines: constraints on their formation from digital elevation model analysis. Tectonics 27:TC3010. https://doi.org/10.1029/2007TC002215
Sarkar A, Patel PP (2011) Topographic analysis of the Dulung R Basin. Indian J Spat Sci II(1):2
Sarkar A, Patel PP (2012) Terrain classification of the Dulung Drainage Basin. Indian J Spat Sci III 1:6
Sarkar A, Roy L, Das S, Sengupta S (2021) Fluvial response to active tectonics: analysis of DEM-derived longitudinal profiles in the Rangit River Basin, Eastern Himalayas India. Environ Earth Sci 80:258. https://doi.org/10.1007/s12665-021-09561-2
Sarkar A, Patel PP (2009) Drainage analysis of the dulung basin. In: Sharma HS, Kale VS (ed) Geomorphology in India. Prayag Pustak Bhavan, Allahabad, pp 133–154
Schumm SA (1956) Evolution of drainage systems and slopes in badlands at Perth Amboy, New Jersey. Geol Soc Am Bull 67:597–646
Searle MP, Owen LA (1999) The evolution of the Indus River in relation to topographic uplift, climate and geology of western Tibet, the Trans-Himalayan and High-Himalayan Range. In: Meadows A, Meadows PS (eds) The Indus River: biodiversity, resources and humankind. Oxford University Press, Oxford, pp 210–230
Seeber L, Gornitz V (1983) River profiles along the Himalayan arc as indicators of active tectonics. Tectonophysics 92:335–367. https://doi.org/10.1016/0040-1951(83)90201-9
Sharma J (2003) Architectural heritage: Ladakh. Haranand Publications, New Delhi
Singh V, Tandon SK (2008) The Pinjaur dun (intermontane longitudinal valley) and associated active mountain fronts, NW Himalaya. Tectonic geomorphology and morphotectonic evolution. Geomorphology 102:376–394. https://doi.org/10.1016/j.geomorph.2008.04.008
Sklar L, Dietrich W (1998) River longitudinal profiles and bedrock incision models: stream power and the influence of sediment supply. In: Tinkler KJ, Wohl EE (eds) Rivers over rocks: fluvial processes in bedrock channels. American Geophysical Union Geophysical Monograph Series, vol 107, pp 207–230
Sofia G (2020) Combining geomorphometry, feature extraction techniques and earth-surface processes research: the way forward. Geomorphology 355:107055. https://doi.org/10.1016/j.geomorph.2020.107055
Strahler AN (1952) Hypsometric (area-altitude) analysis of erosional topography. GSA Bull 63(11):1117–1142
Strahler AN (1957) Quantitative analysis of watershed geomorphology. Trans Am Geophys Union 38(6):913–920. https://doi.org/10.1029/TR038i006p00913
Strecker MR, Hilley GE, Arrowsmith JR, Coutand I (2003) Differential structural and geomorphic mountainfront evolution in an active continental collision zone: the northwest Pamir, southern Kyrgyzstan. Geol Soc Am Bull 115:166–181
Thakur VC (1981) Regional framework and geodynamic evolution of the Indus-Tsangpo suture zone in the Ladakh Himalayas. Trans Royal Soc Edinburgh: Earth Sci 72:87–97
Thayyen RJ, Dimri AP, Kumar P, Agnihotri G (2013) Study of cloudburst and flash floods around Leh, India, during August 4–6, 2010. Nat Hazards 65:2175–2204
Troiani F, Della Seta M (2008) The use of the stream length–gradient index in morphotectonic analysis of small catchments: a case study from Central Italy. Geomorphol 102(1):159–168. https://doi.org/10.1016/j.geomorph.2007.06.020
Wadia, DN (1919) Geology of India. Macmillan Publishers.
Whipple KX (2004) Bedrock rivers and the geomorphology of active orogens. Annu Rev Earth Planet Sci 32:151–185. https://doi.org/10.1146/annurev.32.101802.1203556

Whipple KX, Tucker GE (2002) Implications of sediment flux dependent river incision models for landscape evolution. J Geophys Res-Solid Earth 107:2039. https://doi.org/10.1029/2001JB000162

Wobus CW, Whipple KX, Kirby E, Snyder NP, Johnson J, Spyropolu K, Crosby BT, Sheehan D (2006) Tectonics from topography: procedure, promise and pitfalls. In: Willet SD, Hovius N, Brandon MT, Fisher DM (eds) Tectonics, climate and landscape evolution. Geological Society of America Bulletin Special Paper, vol 398, pp 55–74